NASA TN D-408

TECHNICAL NOTE

D-408

THE BLUNT PLATE IN HYPERSONIC FLOW

By Donald L. Baradell and Mitchel H. Bertram

Langley Research Center
Langley Field, Va.

NATIONAL AERONAUTICS AND SPACE ADMINISTRATION

WASHINGTON

October 1960

NATIONAL AERONAUTICS AND SPACE ADMINISTRATION

TECHNICAL NOTE D-408

THE BLUNT PLATE IN HYPERSONIC FLOW

By Donald L. Baradell and Mitchel H. Bertram

SUMMARY

The sonic-wedge characteristics method has been used to obtain the shock shapes and surface pressure distributions on several blunt two-dimensional shapes in a hypersonic stream for several values of the ratio of specific heats. These shapes include the blunt slab at angle of attack and power profiles of the form $y_b = ax^m$, where $0 < m < 1$, y_b and x are coordinates of the body surface, and a is a constant. These numerical results have been compared with the results of blast-wave theory, and methods of predicting the pressure distributions and shock shapes are proposed in each case.

The effects of a free-stream conical-flow gradient on the pressure distribution on a blunt slab in hypersonic flow were investigated by the sonic-wedge characteristics method and were found to be sizable in many cases. Procedures which are satisfactory for reducing pressure data obtained in conical flows with small gradients are presented.

INTRODUCTION

When a body with a blunt leading edge travels through a fluid at hypersonic speeds, the pressures induced on the afterbody by the blunt leading edge can be of sufficient magnitude to dominate the flow far downstream of the leading edge. In considering such a flow which is dominated by a blunt leading edge it has been found useful to invoke the theory of the decay of intense blast waves (see refs. 1 to 10). Use of a blast-wave analogy has indicated the parameters governing the effect of a blunt leading edge on the pressures and shock shape over a flat plate, and numerical calculations for a slab at zero angle of attack have upheld the correlating power of these parameters (refs. 11 and 12). An examination of the flow similarities which exist behind an intense blast wave indicates that blast-wave theory might also be used in the study of hypersonic flow past certain classes of power bodies (ref. 8).

The pressures induced by the blunt leading edge on a slab at an angle of attack to the stream have been obtained by use of the sonic-wedge

characteristics technique over a range of hypersonic Mach numbers, and an attempt has been made to correlate these results on the basis of the parameters predicted by blast-wave theory. In order to investigate the validity of the blast-wave analogy in the case of power profiles, numerical solutions have been obtained by application of the sonic-wedge leading-edge concept together with rotational characteristics theory as was done in the flat-plate investigation (refs. 11 to 13). The pressure distributions on the power profiles at zero angle of attack have been obtained over a range of hypersonic Mach numbers, and methods of predicting these pressures are presented.

In order to determine the effect of the value of the ratio of specific heats (γ), both the blunt-slab and the power-profile investigation were performed over a range of γ from 1.2 to 1.8, and these results are correlated on the basis of the blast-wave parameters.

Since much hypersonic wind-tunnel testing is performed in conical nozzles which produce a diverging flow with a pressure gradient along the flow axis, the problem of interpreting results obtained in such a nozzle is of prime importance. In order to examine the effect of these external flow gradients on the flow field about a blunt plate and to determine the best method for reducing data obtained in such a flow, the sonic-wedge characteristics method was applied to this problem and numerical solutions were obtained for $\gamma = 5/3$ and $7/5$ at several hypersonic Mach numbers.

SYMBOLS

a	constant
$C_{D,n}$	nose drag coefficient
D_n	nose drag
E	energy
F, f, G	functions of n and γ (see eqs. (1), (3), (5), and (6))
K	blast-wave correlation parameter, $M^3 C_{D,n} \frac{t}{x}$ for planar case
M	Mach number
$M' \equiv \frac{dM}{d(x/t)}$	

m	exponent in power-profile equation ($y \propto x^m$)
n	index number (see eq. (1))
p	static pressure on body surface
R	distance from X-axis to shock
r	distance from origin of source flow
r_n	distance from origin of source flow to nose of model
r_o	distance from origin of source flow to surface along which $M = 1$
$\Delta r = r - r_n$	
s	distance along body axis (see fig. 1(b))
t	nose diameter or leading-edge thickness
U_∞	free-stream velocity
x, y	coordinates (see fig. 1)
α	angle of attack, deg
γ	ratio of specific heats
δ_s	deflection angle which produces sonic flow behind the shock
ϵ	shock angle
θ	flow angle
ρ	density
τ	time

Subscripts:

b	conditions along body surface
l	local conditions
n	free-stream conditions just ahead of model leading edge

sh shock

TW values obtained from tangent-wedge theory

∞ free-stream conditions in uniform flow

THEORETICAL APPROACHES

Blast-Wave Theory

The blast-wave problem, that is the motion and effects of the blast wave produced when a finite amount of energy is suddenly released in an infinitely concentrated form was first discussed by Taylor (ref. 1), who considered the growth of a spherical blast wave. Since then Lin, Sakurai, Lees, Cheng, Chernyi, and others have extended the work of Taylor to include cylindrical and planar waves and have recognized and explored the feasibility of applying the results of blast-wave theory to problems connected with hypersonic flight (refs. 2 to 10). These investigators predict a law of propagation for such intense blast waves which may be expressed as

$$R = F(n,\gamma)\left(\frac{E}{\rho_\infty}\right)^{\frac{1}{3+n}} \tau^{\frac{2}{3+n}} \qquad (1)$$

where

R distance from origin of explosion

ρ_∞ density of undisturbed medium

E energy of blast

τ time

n = 0, 1, or 2 for the planar, cylindrical, or spherical cases, respectively

This formula is expected to predict the shape of the bow shock produced by a blunt-nose (or blunt-leading-edge) body traveling through a fluid at hypersonic speeds in the region not too close to the nose and not so far downstream so that the shock may no longer be considered "strong."

For such a body, if the drag of the nose is much greater than the drag of the afterbody, the energy E may be taken as equal to the drag

of the nose and is therefore effectively constant. Here E has the units of energy/area for the planar case, energy/length for the axisymmetric case, and the energy itself for the spherical case. For the planar case, unit width is considered. For the blunt slab the energy in the flow field about one surface is only one-half the total energy and is therefore taken as one-half the total nose drag. Using these considerations, the formula for E can be written as

$$E = \frac{D_n}{2^{1-n}} = \left(\frac{\pi}{2}\right)^n \frac{\rho_\infty U_\infty{}^2 t^{1+n}}{4} C_{D,n} \tag{2}$$

where

$C_{D,n}$ nose drag coefficient

t nose thickness

n = 0 or 1 for planar or axisymmetric case, respectively

Combining equations (1) and (2) and taking $\tau = x/U_\infty$ there is obtained

$$\frac{R}{t} = f(n,\gamma) C_{D,n}^{\frac{1}{3+n}} \left(\frac{x}{t}\right)^{\frac{2}{3+n}} \tag{3}$$

For a strong shock the pressure distribution behind the shock is given by

$$\frac{p_{sh}}{p_\infty} \approx \frac{2\gamma}{\gamma + 1} M_\infty{}^2 \sin^2\epsilon \approx \frac{2\gamma}{\gamma + 1} M_\infty{}^2 \left[\frac{d(R/t)}{d(x/t)}\right]^2 \tag{4}$$

This equation indicates the limits within which blast-wave theory is expected to apply to hypersonic blunt-body flow fields. The first half of equation (4) holds only for $M_\infty{}^2 \sin^2\epsilon \gg \frac{\gamma - 1}{2\gamma}$; the second half holds only if $\sin^2\epsilon \approx \left[\frac{d(R/t)}{d(x/t)}\right]^2 = \tan^2\epsilon$. Therefore, blast-wave theory is not expected to apply either too far downstream of the nose where the shock is too weak or too close to the nose where the shock is too strong.

When hypersonic similarity applies, p/p_∞ is proportional to p_{sh}/p_∞; therefore, the pressure distribution along the body is given by

$$\frac{p}{p_\infty} = G(n,\gamma)M_\infty{}^2 C_{D,n}{}^{\frac{2}{3+n}} \left(\frac{x}{t}\right)^{-\frac{2(1+n)}{3+n}} \tag{5}$$

For the two-dimensional case considered in this paper equation (5) becomes

$$\frac{p}{p_\infty} = G(\gamma)M_\infty{}^2 C_{D,n}{}^{\frac{2}{3}} \left(\frac{x}{t}\right)^{-\frac{2}{3}} \tag{6}$$

This formula indicates that for any given medium the pressure distributions over blunt slabs at zero angle of attack should correlate on the parameter $K \equiv M_\infty{}^3 C_{D,n} \frac{t}{x}$. An approximate study by Chernyi (refs. 9 and 10) has indicated that the function of γ which should correlate all blunt-slab results at zero angle of attack regardless of the medium is $\sqrt{\gamma(\gamma - 1)}K$; for blunt slabs at angle of attack he found that the pressure parameter $(M_\infty \alpha)^{-2} \frac{p - p_\infty}{p_\infty}$ should correlate against the distance parameter $\frac{s}{t} \frac{\alpha^3}{C_{D,n}}$ where $\frac{s}{t}$ is distance along the body axis.

Lees (ref. 8) has suggested that the blast-wave analogy should also be useful in predicting the flow conditions about certain classes of power bodies where the energy in the flow field is increasing at a constant rate.

The sonic-wedge characteristics method has been applied to each of the aforementioned cases in order to determine the validity of the blast-wave analogy in each case.

The Sonic-Wedge Characteristics Method

When a body is traveling through a fluid at supersonic speeds, the physical properties of the supersonic portion of the flow between the shock which is produced and the body may be calculated numerically by application of the method of characteristics if the boundaries of this supersonic region are known. These calculations are possible whether the flow be considered potential or rotational (ref. 14). In the latter

case the shock-wave equations are combined with the equations of the characteristic system to predict the shape of the curved shock as well as the values of the flow variables in the field behind the shock.

For the case of a body with a blunt leading edge, the supersonic portion of the flow field behind the shock is bounded by the shock, the body surface, and the sonic line - that is, the line extending from the body to the shock which divides the subsonic and supersonic flow regions and along which the Mach number is unity.

L
8
9
7

In the two-dimensional cases considered herein, the computations were simplified by the artifice of replacing the blunt leading edge by a wedge whose inclination is such that the flow everywhere between the shock and the surface of this wedge will be sonic. The sonic line is then a straight line normal to the sonic wedge at the point where this wedge intersects the body, and the flow at all points along the sonic line is normal to the sonic line. Where the sonic wedge intersects the body in question a shoulder is formed and the flow around this shoulder is governed by the Prandtl-Meyer flow relations. When this Prandtl-Meyer expansion is considered as occurring in finite steps, an "expansion fan" is formed and a characteristic net is created by this fan of Mach lines, their "reflections" from the shock, and subsequent reflections from the body in question as shown in the following sketch:

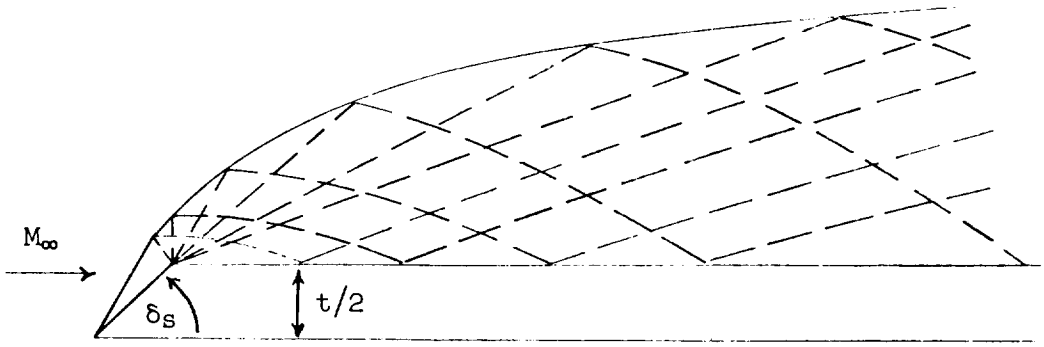

At the shock, the oblique-shock equations are combined with the characteristic equations and the shock strength at any point is computed so as to produce conditions behind the shock consistent with the conditions dictated by the characteristics equations.

In all of the cases considered in this paper the expansion increments were taken as 0.1° for the first degree of the expansion and 1°

thereafter until the expansion is completed. In order to improve the accuracy of the calculations, three iterations were performed at every point. The characteristic computations were performed on an IBM 704 data processing machine.

It has been called to the authors' attention that the manner in which entropy variation is handled in the method used for the characteristics computations can introduce cumulative errors which may become significant at large distances from the leading edge. However, the effects of this inaccuracy on the results presented in this paper are believed to be insignificant.

RESULTS OF NUMERICAL CALCULATIONS

The Blunt Slab in Uniform Flow

The sonic-wedge characteristics method has been applied to determine the pressure distribution on a blunt slab situated in a hypersonic stream as shown in figure 1(a). Results for the case of zero angle of attack for values of γ of 5/3 and 7/5 and a range of hypersonic Mach numbers have been presented in references 11 to 13. In reference 9, Chernyi has obtained by an approximate analysis the parameter which governs the effect of the value of the ratio of specific heats γ on the pressures dictated by blast-wave theory. In order to check the correlating power of this parameter, solutions have been obtained by the sonic-wedge characteristics method for a blunt slab at zero angle of attack for Mach numbers of 9.5 and 20 and values of γ of 6/5, 7/5, 5/3, and 9/5, and the results are presented in figure 2, which presents the pressure difference ratio plotted against the parameter given by Chernyi. Although the basic assumptions in the derivation by Chernyi are more exact as $\gamma \to 1$ certain steps in the derivation require that $\gamma - 1$ be not too close to 0. It is seen in figure 2 that for the higher values of γ (5/3 and 9/5) the correlation is excellent. However, for $\gamma = 7/5$ the deviation from correlation is about 3 percent and for $\gamma = 6/5$, 10 to 15 percent. Thus the correlation suggests that for the function of γ suggested by Chernyi to be valid in application $\gamma - 1$ must be greater than about 1/2. The curve which correlates the results for the higher values of γ is

$$\frac{p - p_\infty}{p_\infty} = 0.187\left[\sqrt{\gamma}(\gamma - 1)\,\frac{M_\infty^3 C_{D,r}}{x/t}\right]^{2/3} - 0.26 \qquad (7)$$

In order to obtain accurate results for $\gamma < 5/3$ this correlation curve may be raised slightly by the percentage factor indicated in figure 2.

For the case of a blunt plate at angle of attack to a hypersonic stream, the governing parameter has again been suggested by Chernyi in references 9 and 10 where he shows that $(M_\infty\alpha)^{-2}\frac{p - p_\infty}{p_\infty}$ is a function of $\frac{s}{t}\frac{\alpha^3}{C_{D,n}}$. Results have been obtained by the sonic-wedge characteristics method for a blunt slab at angle of attack as shown in figure 1(b) for a wide range of Mach numbers and angles of attack and for $\gamma = 5/3$ and $7/5$. For this investigation the sonic wedge was kept alined with the stream as shown in figure 1(b). These results are presented in figure 3 where it can be seen that the parameter does a fair job of correlating the pressure distributions on the high-pressure side of the slab ($\alpha > 0^\circ$) but has poor overall success correlating the pressures on the low-pressure side ($\alpha < 0^\circ$). On the high-pressure side for the lowest value of $M_\infty\alpha$ presented the deviation from correlation is considerable; therefore, an attempt was made to determine whether the distributions for small angles of attack might be given by a simple linear addition of the pressure predicted by tangent-wedge theory and the pressure increment due to a blunt leading edge on a slab at zero angle of attack. If this were the case, then

$$\frac{p - p_\infty}{p_\infty} - \left(\frac{p - p_\infty}{p_\infty}\right)_{TW} = \left(\frac{p - p_\infty}{p_\infty}\right)_{\text{Blunt slab}(\alpha=0^\circ)} \tag{8}$$

These values are presented in figure 4 for Mach numbers of 9.5 and 20; $\gamma = 7/5$; and $\alpha = 0^\circ, \pm1^\circ, \pm3^\circ, \pm5^\circ$, and $\pm10^\circ$. As can be seen, this linear addition does a fair job of predicting the distribution for angles of attack in the range $-1^\circ < \alpha < +3^\circ$ and any application of this method must be limited to this range. For values of $\alpha > 3^\circ$ however, the pressure distributions correlate well on the basis of the parameters indicated by Chernyi; therefore, the entire positive angle-of-attack range is covered by these methods.

Examples of the shock shapes obtained in this investigation are presented in figure 5 where it is seen that the shape is independent of the angles of attack for several leading-edge thicknesses back from the leading edge of the model for angles of attack up to 10° to 20°.

For the positive angles of attack the shock shape must undergo a transition from the shape induced by the blunt leading edge to the shape induced by the afterbody which must be of the form $\frac{R}{t} \propto \frac{x}{t}$. This transition is seen to begin nearer to the leading edge as the angle of attack of the afterbody is increased.

Note that the shock shapes are identical for all negative angles of attack for as far back as the calculations go. This is due to the fact that for these cases the calculations are terminated before any reflections from the body downstream of the shoulder can reach the shock. The shock shape is therefore a product only of the initial shoulder expansion fan.

Power Profiles in Uniform Flow

When the hypersonic-flow equations are examined in the light of blast-wave theory, it is found that flow similarity can exist for bodies of the form $\left(\frac{y_b}{t}\right) \propto \left(\frac{x}{t}\right)^m$ for certain values of the exponent m (ref. 8). The range of these permissible values is $\frac{2}{3+n} \leqq m \leqq 1$, where $n = 0$ for planar flow and $n = 1$ for axially symmetric flow. When this similarity exists the shock wave is expected to be of the form $\left(\frac{R}{t}\right) \propto \left(\frac{x}{t}\right)^m$ and from equations (4) and (5) it is seen that the pressure distribution along the body is given by

$$\frac{p}{p_\infty} \propto M_\infty{}^2\left(\frac{x}{t}\right)^{-2(1-m)} \propto M_\infty{}^2 \tan^2\theta_b \tag{9}$$

where $\tan \theta_b$ is the local body slope.

In order to check the existence of these similarities in the two-dimensional case, the sonic-wedge characteristics method was applied to the problem. The bodies considered were of the family

$$\frac{y_b}{t} = 2^{m-1}(\tan \delta_s)^m\left(\frac{x}{t}\right)^m$$

where δ_s is the sonic-wedge angle.

The sonic wedge then starts from the vertex of the profile in question and intersects the profile at $\frac{y}{t} = \frac{1}{2}$ as shown in the sketch in figure 1(c). Values of m considered were 1/4, 1/2, 2/3, 3/4, and 7/8 for Mach numbers of 10, 20, and 40 and $\gamma = 6/5$, 7/5, 5/3, and 9/5.

Some shock shapes obtained by this method are presented in figure 6. As was previously mentioned, for bodies such that $\frac{2}{3} \leqq m \leqq 1$ the shock shape should be given by $\frac{R}{t} \propto \left(\frac{x}{t}\right)^m$. From the blunt-leading-edge flat-plate studies (corresponding to $m = 0$), it was found that the shock shape is given roughly by $\left(\frac{R}{t}\right) \propto \left(\frac{x}{t}\right)^{2/3}$. Therefore, not much change in shock shape is expected in the range $0 \leqq m \leqq \frac{2}{3}$; this, as may be seen in figure 6, is at least approximately true. For the bodies such that $\frac{2}{3} \leqq m \leqq 1$, it is seen that the shape of the shock is a strong function of the power of the body, so that the type of flow similarity predicted by blast-wave theory does seem to exist roughly in the cases considered herein.

The results of the pressure investigation, presented in figure 7, indicate that as far as surface pressures are concerned, flow similarity does exist to a certain extent for bodies in the range $\frac{2}{3} \leqq m \leqq 1$. Also shown in this figure is the pressure distribution as predicted by tangent-wedge theory, which is seen to agree very well with the characteristics results for the $m = 7/8$ profile and to agree roughly with the distributions obtained for $m = 2/3$ and $3/4$.

It was also found, as shown in figure 8, that even a substantial change in the value of the ratio of specific heats has little effect on the rate of pressure decay along the body for all cases considered herein. The function of gamma shown in the ordinate is that suggested by first-order tangent-wedge theory for large values of $M_\infty \tan \alpha$.

For the higher power bodies ($m \geqq 2/3$) hypersonic tangent-wedge theory predicts the pressure distributions quite accurately in the range in which it would be expected to apply. This fact is shown in figure 9 where the pressure distributions on a typical higher power profile ($m = 3/4$) and a typical lower power profile ($m = 1/4$) are presented for $\gamma = 7/5$ and several Mach numbers. The abscissa in this figure is the reciprocal of the hypersonic similarity parameter. While the pressure distributions for the $m = 3/4$ profile are seen to correlate well when plotted against this parameter, no correlation exists for the $m = 1/4$ profile.

The bodies for which $0 < m < 2/3$ exhibit no similarity but the pressure distribution along these bodies may be satisfactorily predicted

by a linear addition of the pressures predicted by exact tangent-wedge theory and the blunt-leading-edge increment obtained for the slab at $\alpha = 0^\circ$. As seen in figure 10 this linear addition predicts the pressure distribution quite satisfactorily for the more slender profiles considered herein (m = 1/2 and 1/4). This suggests that for any slender convex profile with a blunt leading edge, the pressures may be predicted by the relation

$$\frac{p}{p_\infty} = \left(\frac{p}{p_\infty}\right)_{TW} + \left(\frac{p - p_\infty}{p_\infty}\right)_{\text{Blunt slab}(\alpha=0^\circ)} \tag{10}$$

where $\left(\frac{p}{p_\infty}\right)_{TW}$ is the exact tangent-wedge value and $\left(\frac{p - p_\infty}{p_\infty}\right)_{\text{Blunt slab}(\alpha=0^\circ)}$ is the pressure increment on a slab ($\alpha = 0^\circ$) due to the blunt leading edge; this increment may be obtained from figure 2.

The Blunt Slab in Nonuniform Flow

Since much hypersonic wind-tunnel testing is done in conical nozzles which produce a diverging flow with a pressure gradient along the nozzle axis, the problem of interpreting results obtained in such a nozzle is of prime importance. Figure 11 illustrates the problem encountered by presenting experimental data obtained in a uniform flow nozzle where the Mach number in the test region was 11.6 and experimental data obtained in a conical-flow nozzle where the Mach number at the leading edge of the model was 11.6. Both of these sets of data were obtained on a flat-face slab in the Princeton University helium hypersonic tunnel and were taken from figure 5 of reference 15. The data obtained in the conical nozzle are presented twice corresponding to two methods that have been used in reducing the data obtained in conical nozzles. These methods correspond to the cases where either local free-stream static pressure or free-stream static pressure at the nose are used to normalize the wall pressures. These methods will be discussed in more detail later. Also presented in figure 11 are the distributions obtained by the sonic-wedge characteristics theory employed in the present investigation as outlined later. Since the characteristics results have been obtained for a sonic-wedge leading edge, the abscissa in figure 11 has been adjusted by the ratio of the nose drag coefficients as suggested by blast-wave theory. It may be seen from figure 11 that experimental and theoretical results are in essential agreement and the problem of the effect of nozzle flow gradients on measured pressures can assume serious proportions.

In order to examine the effects of these external flow gradients on the flow field about a blunt slab, the sonic-wedge characteristics method was applied to this problem as shown in figure 1(d).

The nozzle flow field was considered to obey the laws of conical-source flow. For this type flow, the following equation is obtained from the area ratio equation

$$\frac{r}{r_o} = \frac{1}{M^{1/2}}\left[\frac{2}{\gamma + 1}\left(1 + \frac{\gamma - 1}{2} M^2\right)\right]^{\frac{\gamma+1}{4(\gamma-1)}} \tag{11}$$

where r is the distance from the fictitious origin of the conical-source flow and r_o is the distance from the fictitious flow origin to the spherical surface along which $M = 1$, as shown in the following sketch:

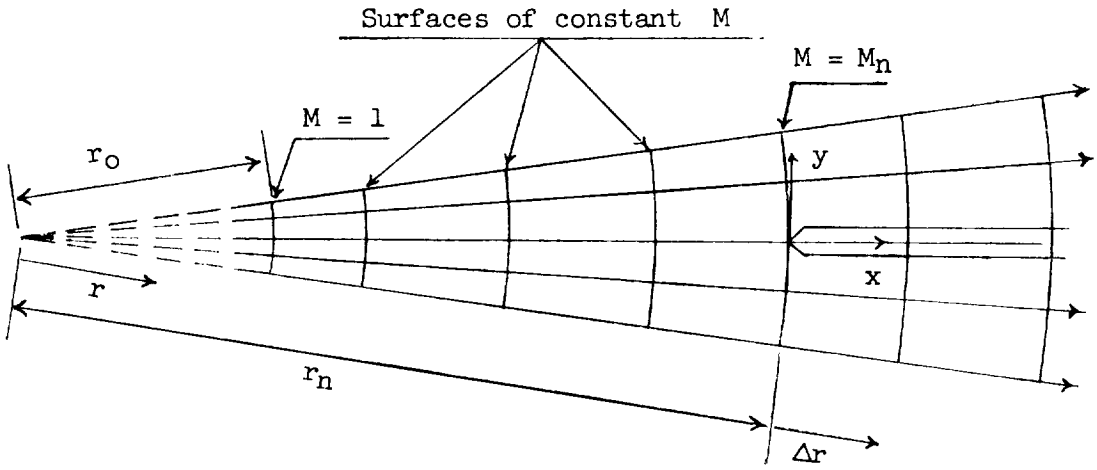

Differentiating equation (11) gives the Mach number gradient as

$$M' \equiv \frac{dM}{dr/t} = \frac{(\gamma + 1)M^{3/2}}{r_o/t\left(M^2 - 1\right)}\left[\frac{2}{\gamma + 1}\left(1 + \frac{\gamma - 1}{2} M^2\right)\right]^{\frac{3\gamma-5}{4(\gamma-1)}} \tag{12}$$

where t is the model leading-edge thickness. Equation (12) gives the Mach number gradient per leading-edge thickness as a function of

the local Mach number M, the ratio of specific heats for the test medium γ, and the characteristic length r_o which is now evaluated.

For a given Mach number and Mach number gradient at the leading edge of a model, designated as M_n and M_n', respectively, from equations (11) and (12) the values for r_o/t and r_n/t are obtained, where r_n is the value of r at the leading edge. These values are

$$\frac{r_o}{t} = \frac{(\gamma + 1)M_n^{3/2}}{\left(M_n^2 - 1\right)} \frac{1}{M_n'} \left[\frac{2}{\gamma + 1} \left(1 + \frac{\gamma - 1}{2} M_n^2 \right) \right]^{\frac{3\gamma - 5}{4(\gamma - 1)}} \tag{13}$$

and

$$\frac{r_n}{t} = \frac{2M_n}{M_n^2 - 1} \left(1 + \frac{\gamma - 1}{2} M_n^2 \right) \frac{1}{M_n'} \tag{14}$$

For helium ($\gamma = 5/3$) equations (13) and (14) reduce to

$$\left.\begin{aligned} \frac{r_o}{t} &= \frac{8M_n^{3/2}}{3\left(M_n^2 - 1\right)} \frac{1}{M_n'} \\ \frac{r_n}{t} &= \frac{2}{3} \frac{M_n\left(M_n^2 + 3\right)}{M_n^2 - 1} \frac{1}{M_n'} \end{aligned}\right\} \tag{15}$$

and for air ($\gamma = 7/5$),

$$\left.\begin{aligned} \frac{r_o}{t} &= \frac{12}{5} \frac{M_n^{3/2}}{\left(M_n^2 - 1\right)\left(\frac{6}{M_n^2 + 5}\right)^{1/2}} \frac{1}{M_n'} \\ \frac{r_n}{t} &= \frac{2}{5} \frac{M_n\left(M_n^2 + 5\right)}{M_n^2 - 1} \frac{1}{M_n'} \end{aligned}\right\} \tag{16}$$

Since equation (11) is at best a quartic in M, the problem was simplified by taking the Mach number gradient in the flow field beyond the leading edge as constant and equal to the Mach number gradient at the leading edge. The Mach number in the undisturbed nozzle flow is then given by

$$M = M_n + M_n'\left(\frac{\Delta r}{t}\right) \tag{17}$$

where $\Delta r/t = \frac{r - r_n}{t}$. The extent of the validity of this approximation may be seen in figure 12, where the percentage Mach number change in the undisturbed flow and the ratio of the local stream static pressure in the undisturbed flow to the stream static pressure just ahead of the model leading edge are plotted against the parameter dictated by equation (17). The agreement between the exact conical-flow values and the values obtained by the method used in the present investigation is seen to be very good up to a value of $\frac{M_n'}{M_n}\frac{\Delta r}{t}$ of about 0.1 for $\gamma = 5/3$ and 0.05 for $\gamma = 7/5$. This indicates that the results presented in this paper are applicable to true conical-source flow as long as the Mach number change along the model axis is on the order of one-tenth the stream Mach number or less.

The flow angle at any point in the undisturbed flow is obtained from the relation $\sin\theta = y/r$ where y is the normal distance from the flow axis of symmetry. If the X-axis is taken along the flow axis of symmetry with origin at the model leading edge, then

$$\frac{r}{t} = \sqrt{\left(\frac{r_n}{t} + \frac{x}{t}\right)^2 + \left(\frac{y}{t}\right)^2} \tag{18}$$

and

$$\theta = \tan^{-1}\left(\frac{y/t}{\frac{x}{t} + \frac{r_n}{t}}\right) \tag{19}$$

In order to determine whether the flow angles present in the test regions of conical nozzles, though small (usually less than 1°) have any significant effects on the measured pressures, three characteristics solutions were obtained for a leading-edge Mach number of 11.5.

In one case the flow was considered uniform with $M' = 0$ and $\theta = 0$ everywhere in the undisturbed stream. The next case considered a pressure gradient $\left(M_n' = 0.02\right)$ but neglected flow angularity, considering $\theta = 0$ everywhere in the undisturbed stream. This is the approach that was taken in reference 16. In the third case the flow field was considered to have $M_n' = 0.02$ as in the previous case but the flow angle in the undisturbed stream was taken as given by equation (19). The results of this investigation, presented in figure 13, show that in the case considered the effects of the flow divergence on the measured pressure distribution are at least of the same order as the effects of the pressure gradient. All other results obtained in this investigation, therefore, consider both the effects of flow angularity and pressure gradient on the surface pressure distribution.

Numerical results have been obtained for $\gamma = 5/3$ at $M_n = 10$ and 20 and for $\gamma = 7/5$ at $M_n = 20$. Values of M_n' of 0.01, 0.02, 0.05, 0.10, and 0.20 were considered in each case. These results are presented in figures 14 and 15.

Several methods for reducing results obtained in conical nozzles have been proposed. One method is just to neglect the effects of the flow gradients and say simply that

$$\left(\frac{p}{p_n}\right)_{\text{Conical flow}} = \left(\frac{p}{p_\infty}\right)_{\text{Uniform flow}} \tag{20}$$

where p_n is the static pressure just ahead of the nose in a conical-flow nozzle and p_∞ is the static pressure in a uniform-flow nozzle. As may be seen from figures 11, 13, 14, and 15 the pressure distributions thus obtained are considerably below the uniform flow pressure distributions. A second method proposes taking the ratio of the measured pressure to the local stream static pressure in the undisturbed stream p_l. That is

$$\left(\frac{p}{p_l}\right)_{\text{Conical flow}} = \left(\frac{p}{p_\infty}\right)_{\text{Uniform flow}} \tag{21}$$

As may be seen from figures 14 and 15 this method overcorrects for the gradient and gives a distribution considerably higher than the uniform-flow distribution. In both of these methods the deviation from

the uniform-flow distribution increases as the leading-edge Mach number decreases, as the magnitude of the gradient increases, or as the distance from the leading edge increases.

By analogy to the linear addition method used in the power-profile investigation, a method of linear addition suggests itself in this case. Here the pressure increment induced by the nozzle pressure gradient should be added to the uniform-flow pressure distribution. This approach, which is identical to the "buoyancy" correction used in references 16 and 17 says simply that

$$\left(\frac{p}{p_n}\right)_{\text{Conical flow}} = \left(\frac{p}{p_\infty}\right)_{\text{Uniform flow}} + \left(\frac{p_l - p_n}{p_n}\right)_{\text{Conical flow}} \tag{22}$$

If this approach is correct then when the pressures obtained in the conical nozzle are adjusted by the subtraction of this increment the results should agree with the uniform-flow results. That is

$$\left(\frac{p}{p_n}\right)_{\text{Conical flow}} - \left(\frac{p_l - p_n}{p_n}\right)_{\text{Conical flow}} = \left(\frac{p}{p_\infty}\right)_{\text{Uniform flow}} \tag{23}$$

The pressure distributions obtained for the conical-flow cases and reduced by this linear addition method are presented in figures 14 and 15 and are seen to be in better agreement with the uniform-flow distribution than the distributions obtained by the other methods presented for all cases considered.

Although this correction is satisfactory for the smaller gradient cases considered, examination of the figures indicates that this correction is insufficient when the product $M_n M_n'$ is greater than about 0.5. It should be mentioned that these large gradients M_n' can be encountered in testing a model with a large leading-edge thickness in a flow field whose absolute gradient may be small.

Due to the success of blast-wave theory in the correlation of uniform-flow free-stream blunt-slab results, the idea of modifying the blast-wave-theory parameters to correlate the conical-flow results was investigated. The first-order modified pressure relation is given by

$$\frac{p}{p_l} \propto M_l^2 C_{D,n}^{2/3} \left(\frac{x}{t}\right)^{-2/3} \tag{24}$$

These parameters are presented in figure 16 for values of M_n of 10 and 20 and $\gamma = 5/3$. Also shown in this figure for purposes of comparison is the uncorrected conical-flow distribution for which p/p_n is plotted against $K_n^{-1} \equiv \frac{1}{M_n^3 C_{D,n}} \frac{x}{t}$. As may be seen in figure 16 the distribution given by equation (21) agrees favorably with the uniform-flow results for values of $\frac{M_n'}{M_n} < 0.05$ for $M_n = 10$ and 20.

CONCLUDING REMARKS

The pressure distributions on blunt slabs at zero angle of attack to the flow direction in any testing medium correlate well on the basis of parameters dictated by blast-wave theory in the range where blast-wave theory is expected to apply.

For a blunt plate at an angle of attack, the pressure distributions correlate fairly well on the basis of blast-wave-theory parameters for values of angle of attack $\alpha \geq 3^\circ$ for Mach number $M > 5$. For values of α in the range $-1 < \alpha < 3^\circ$ the pressure distributions can be satisfactorily predicted by a linear addition of the pressures predicted by tangent-wedge theory and the pressure increment induced by the blunt leading edge on a slab at zero angle of attack. For values of $\alpha < -1^\circ$ attempts to correlate or predict pressure distributions met with little success.

For a blunt slab at zero angle of attack the shock shapes agree fairly well with the prediction of blast-wave theory. For positive angles of attack ($\alpha > 0^\circ$) the shock shapes undergo a transition from the shape produced by the blunt leading edge to the shape produced by the wedge-like afterbody, with this transition starting sooner as α is increased.

The shock shapes produced by profiles of the form $y_b = ax^m$ do appear to be proportional to the body shape for $2/3 \leq m \leq 1$ as

predicted by blast-wave theory. (The symbols y_b and x are coordinates of the body surface and a is a constant.) There is little change in the shock shapes produced by power profiles in the range $0 \leqq m \leqq 2/3$. Pressure distributions obtained on these power profiles indicate that flow similarity does exist to a certain extent for bodies in the range $2/3 \leqq m \leqq 1$ as predicted by blast-wave theory. For $0 \leqq m \leqq 2/3$ no similarity has been found but the pressure distributions may be satisfactorily predicted by a linear addition of the pressures predicted by tangent-wedge theory and the pressure increment induced by the blunt leading edge on a slab at zero angle of attack. This result suggests that this method of linear addition should be applicable to obtain the pressure distribution on any slender convex profile with a blunt leading edge in a hypersonic stream.

When testing in conical nozzles it should be remembered that the effects of nozzle flow gradients on measured pressures can assume serious proportions. A simple and satisfactory method for reducing pressures measured in nozzles with small gradients is the linear addition of the measured pressures and the static pressure increment due to the nozzle flow gradient.

When the blast-wave parameters are based on local conditions the pressure distributions obtained are found to agree with the distributions encountered in the uniform flow case up to a value of $\frac{M_n'}{M_n}\frac{x}{t}$ of about 0.05 for $M_n = 10$ and 20, where M_n and M_n' are the Mach number and the Mach number gradient at the nose of the model, respectively, and t is the model thickness.

No satisfactory method has been yet found for interpreting results obtained in flows with large gradients.

Langley Research Center,
National Aeronautics and Space Administration,
Langley Field, Va., July 29, 1960.

REFERENCES

1. Taylor, Geoffrey: The Formation of a Blast Wave by a Very Intense Explosion. Proc. Roy. Soc. (London), ser. A, vol. 201, no. 1065, Mar. 22, 1950.
   I. Theoretical Discussion, pp. 159-174.
   II. The Atomic Explosion of 1945, pp. 175-186.

2. Lin, Shao-Chi: Cylindrical Shock Waves Produced by Instantaneous Energy Release. Jour. App. Phys., vol. 25, no. 1, Jan. 1954, pp. 54-57.

3. Sakurai, Akira: On the Propagation and Structure of the Blast Wave, I. Jour. Phys. Soc. of Japan, vol. 8, no. 5, Sept.-Oct. 1953, pp. 662-669.

4. Sakurai, Akira: On the Propagation and Structure of a Blast Wave, II. Jour. Phys. Soc. of Japan, vol. 9, no. 2, Mar.-Apr. 1954, pp. 256-266.

5. Cheng, Hsien K.: Similitude of Hypersonic Real-Gas Flows Over Slender Bodies With Blunted Noses. Jour. Aero/Space Sci., vol. 26, no. 9, Sept. 1959, pp. 575-585.

6. Cheng, H. K., and Pallone, A. J.: Inviscid Leading-Edge Effect in Hypersonic Flow. Jour. Aero. Sci. (Readers' Forum), vol. 23, no. 7, July 1956, pp. 700-702.

7. Cheng, H. K., Hall, J. Gordon, Golian, T. C., and Hertzberg, A.: Boundary-Layer Displacement and Leading-Edge Bluntness Effects in High-Temperature Hypersonic Flow. Paper No. 60-38, Inst. Aero. Sci., Jan. 1960.

8. Lees, Lester, and Kubota, Toshi: Inviscid Hypersonic Flow Over Blunt-Nosed Slender Bodies. Jour. Aero. Sci., vol. 24, no. 3, Mar. 1957, pp. 195-202.

9. Chernyi, G. G.: Hypersonic Flow Past an Airfoil With a Slightly Blunted Leading Edge. C-112, Morris D. Friedman, Inc. (Needham Heights 94, Mass.). (From Doklady Akademii Nauk USSR, vol. 114, no. 4, 1957, pp. 721-724.)

10. Chernyi, G. G.: Effect of Slight Blunting of Leading Edge of an Immersed Body on the Flow Around It at Hypersonic Speeds. NASA TT F-35, 1960.

11. Bertram, M. H., and Baradell, D. L.: A Note on the Sonic-Wedge Leading-Edge Approximation in Hypersonic Flow. Jour. Aero. Sci. (Readers' Forum), vol. 24, no. 8, Aug. 1957, pp. 627-629.

12. Bertram, Mitchel H., and Henderson, Arthur, Jr.: Effects of Boundary-Layer Displacement and Leading-Edge Bluntness on Pressure Distribution, Skin Friction, and Heat Transfer of Bodies at Hypersonic Speeds. NACA TN 4301, 1958.

13. Bertram, Mitchel H.: Viscous and Leading-Edge Thickness Effects on the Pressures on the Surface of a Flat Plate in Hypersonic Flow. Jour. Aero. Sci. (Readers' Forum), vol. 21, no. 6, June 1954, pp. 430-431.

14. Ferri, Antonio: Application of the Method of Characteristics to Supersonic Rotational Flow. NACA Rep. 841, 1946. (Supersedes NACA TN 1135.)

15. Vas, I. E., and Bogdonoff, S. M.: Hypersonic Studies of Blunt Unswept Wings. Rep. No. 450 (WADC TN 59-127, AD 214 623), Dept. Aero. Eng., Princeton Univ., Apr. 1959.

16. Mueller, James N., Close, William H., and Henderson, Arthur, Jr.: An Investigation of Induced-Pressure Phenomena on Axially Symmetric, Flow-Alined, Cylindrical Models Equipped With Different Nose Shapes at Free-Stream Mach Numbers From 15.6 to 21 in Helium. NASA TN D-373, 1960.

17. Love, Eugene S., Coletti, Donald E., and Bromm, August F., Jr.: Investigation of the Variation With Reynolds Number of the Base, Wave, and Skin-Friction Drag of a Parabolic Body of Revolution (NACA RM-10) at Mach Numbers of 1.62, 1.93, and 2.41 in the Langley 9-Inch Supersonic Tunnel. NACA RM L52H21, 1952.

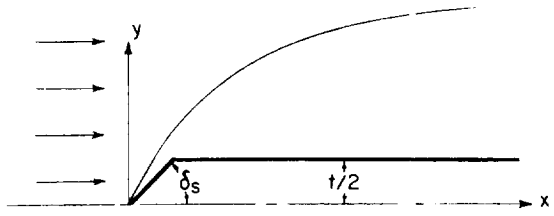

(a) Blunt flat plate at zero angle of attack.

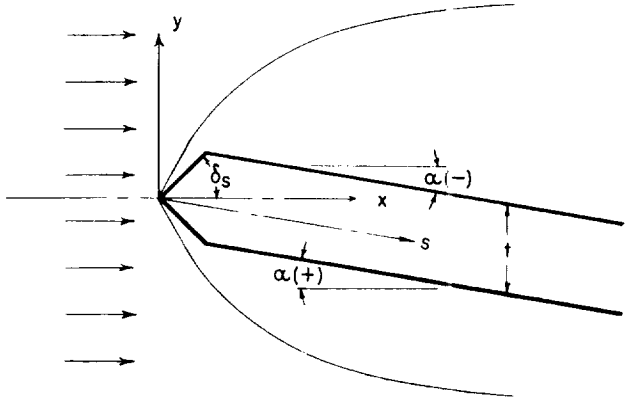

(b) Blunt flat plate at angle of attack.

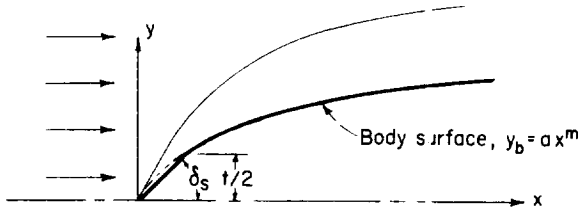

(c) Power profile.

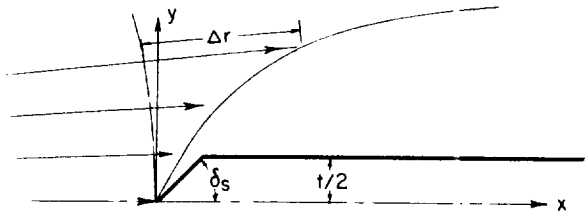

(d) Blunt flat plate in nonuniform flow.

Figure 1.- Sketches illustrating the various models used for the numerical computations.

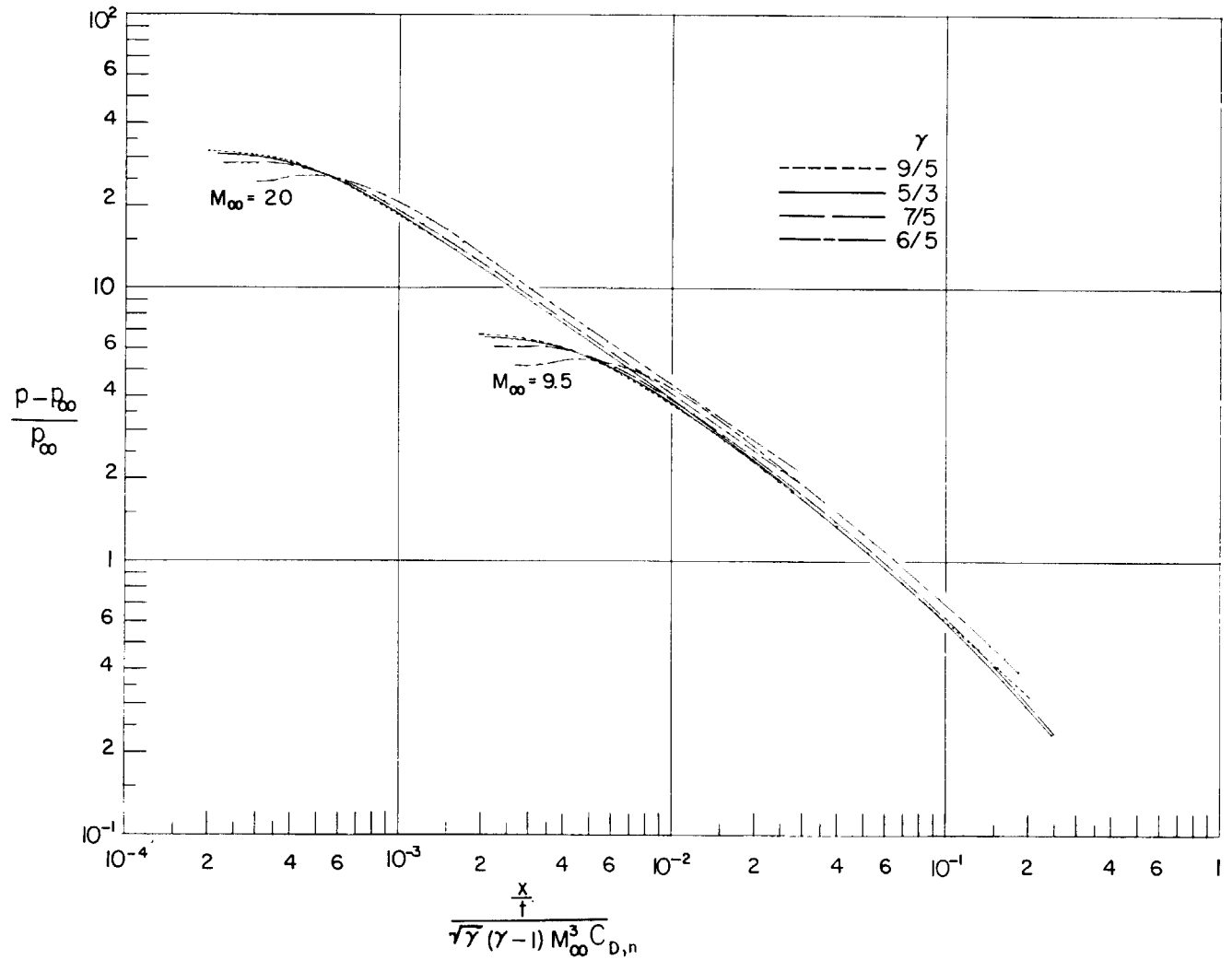

Figure 2.- Correlation of pressures on a slab induced by blunt leading edge including the effect of the ratio of specific heats. $\alpha = 0^\circ$.

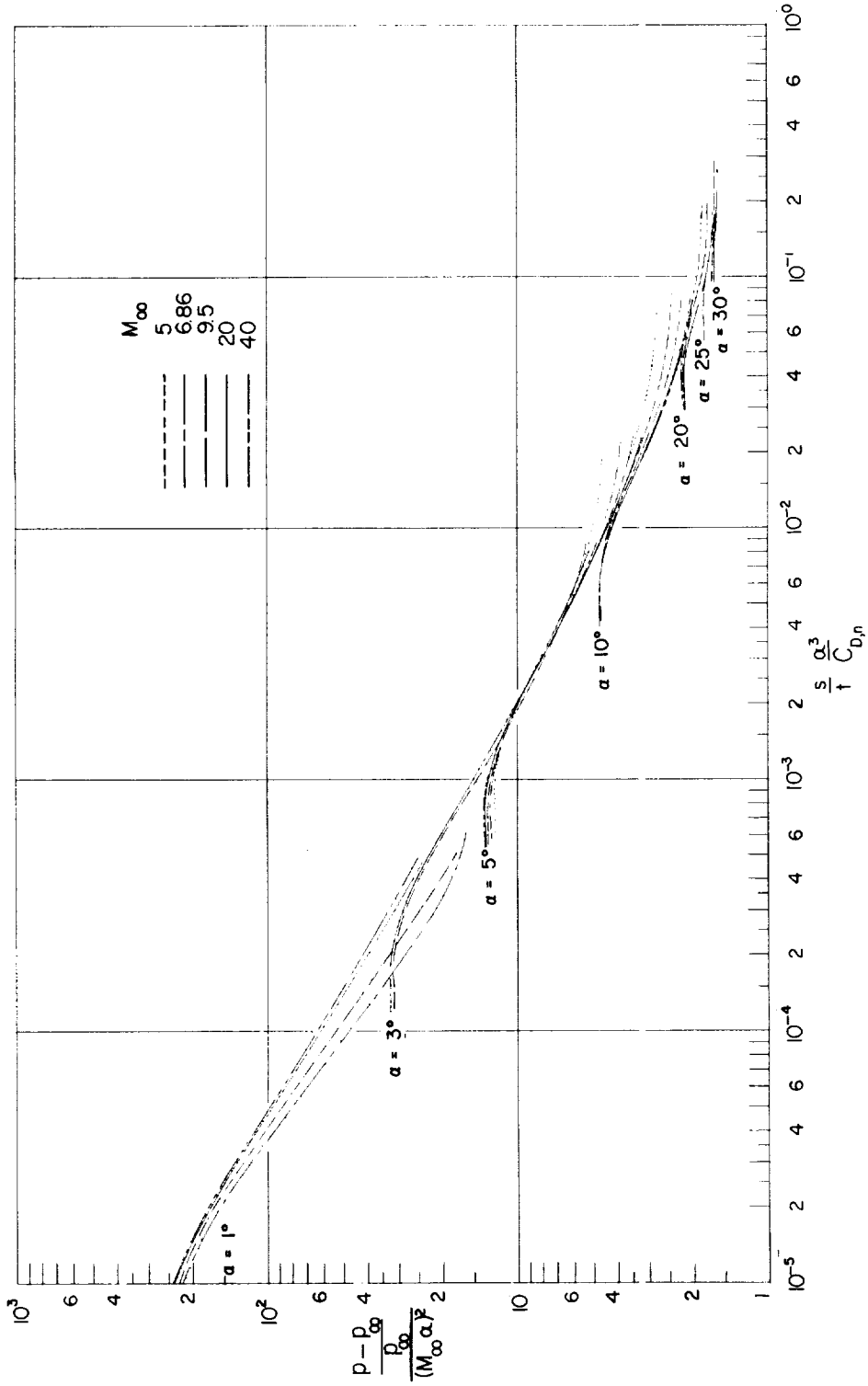

(a) Windward surface; $\gamma = 7/5$.

Figure 3.- Correlation according to blast-wave theory of pressures on a blunt-leading-edge slab.

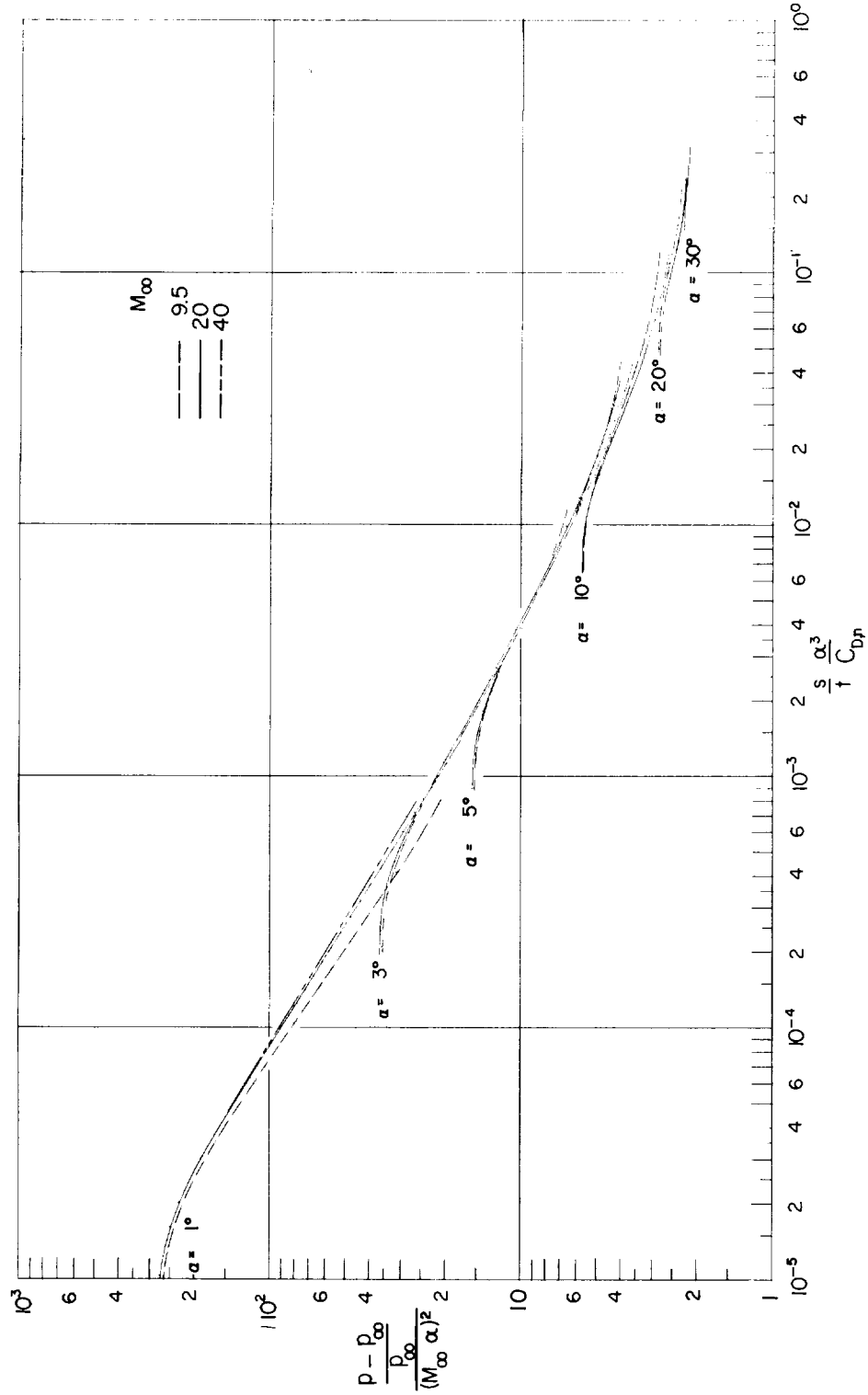

(b) Windward surface; $\gamma = 5/3$.

Figure 3.- Continued.

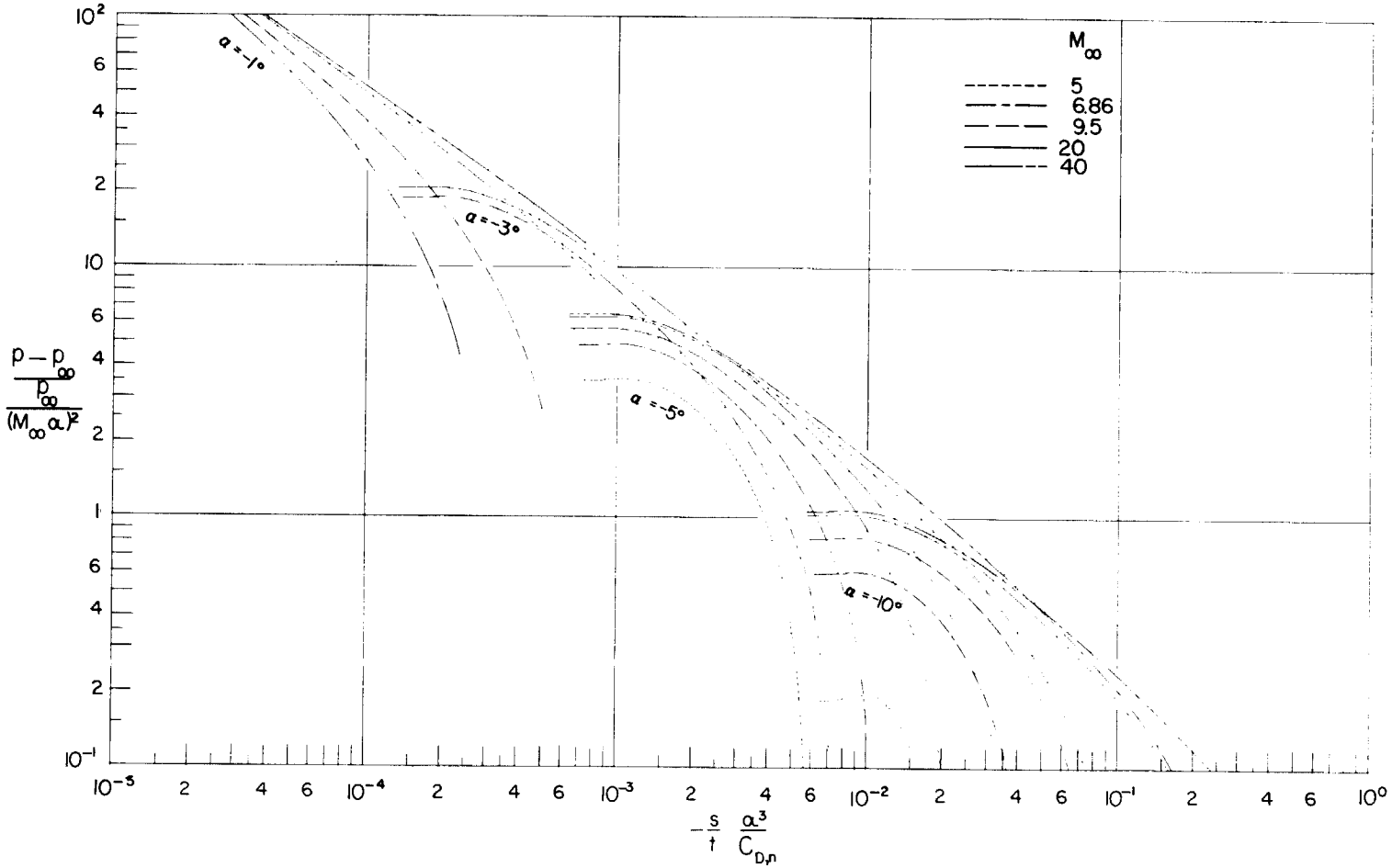

(c) Leeward surface; $\gamma = 7/5$.

Figure 3.- Continued.

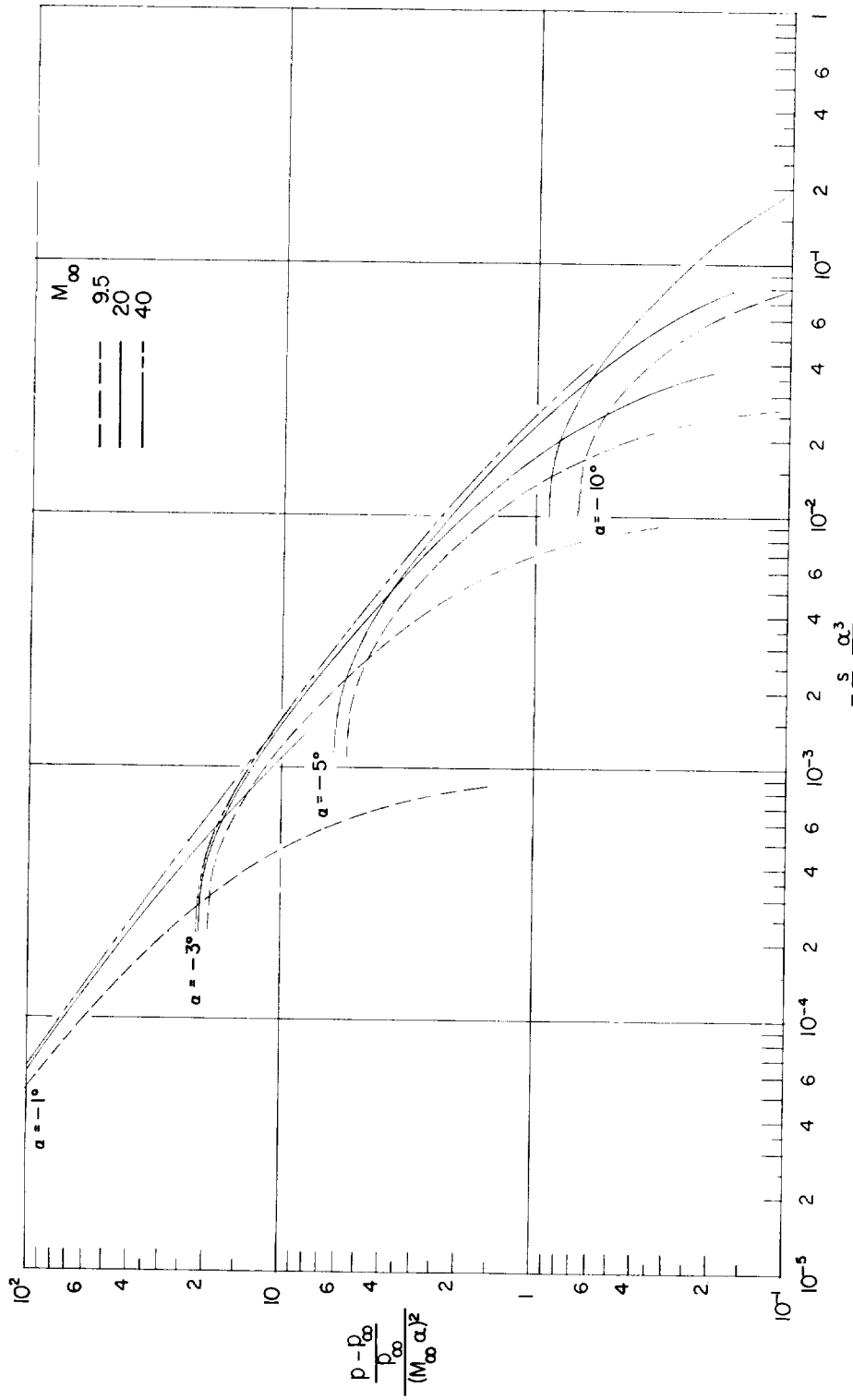

(d) Leeward surface; $\gamma = 5/3$.

Figure 3.- Concluded.

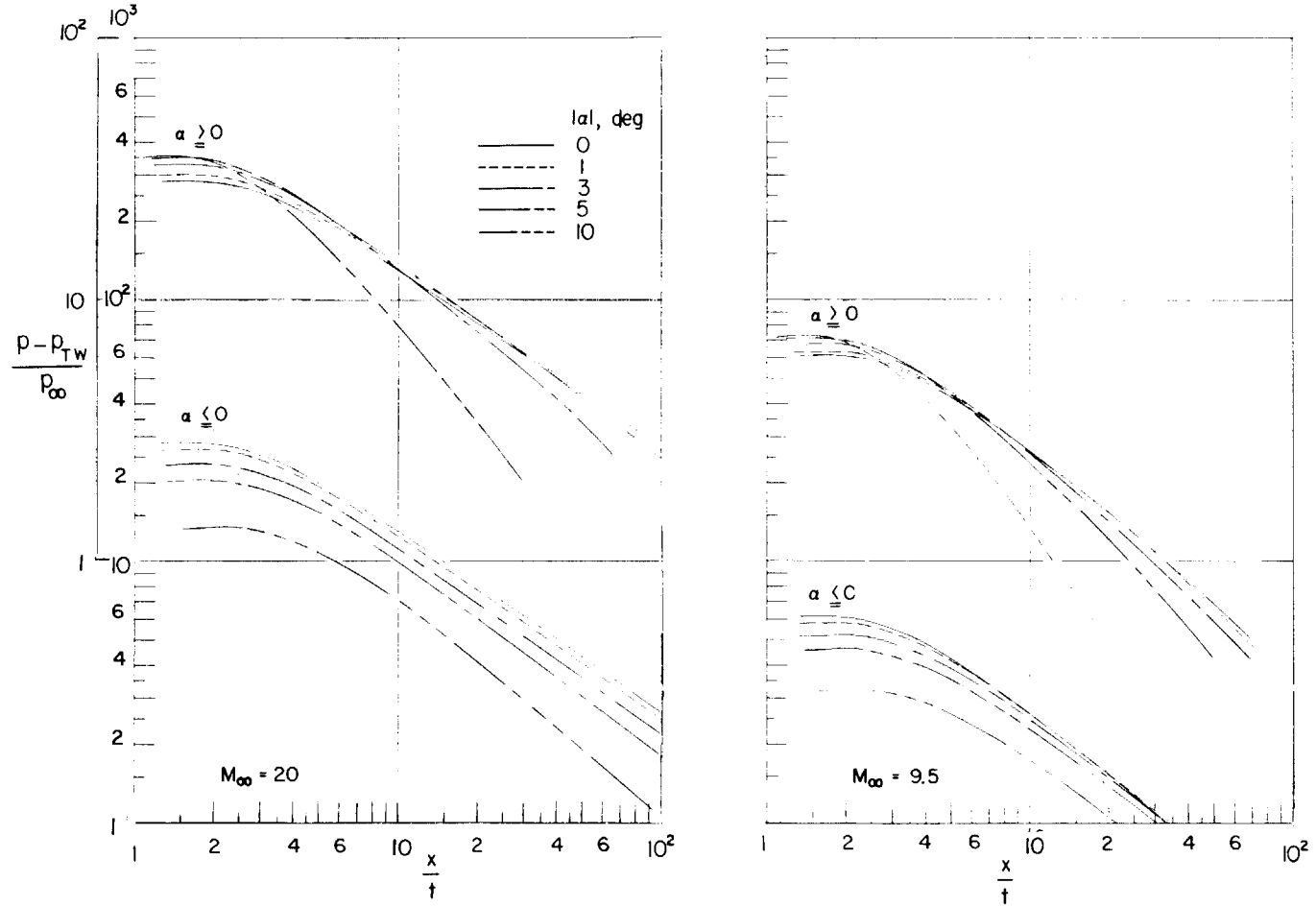

Figure 4.- Comparison of surface pressure on blunt-leading-edge slab at zero inclination to uniform stream and the slab at small angles of attack where pressure parameter in ordinate is obtained by linear addition of calculated blunt slab pressures at angle of attack and pressure for sharp-leading-edge wing at same angle of attack. $\gamma = 7/5$.

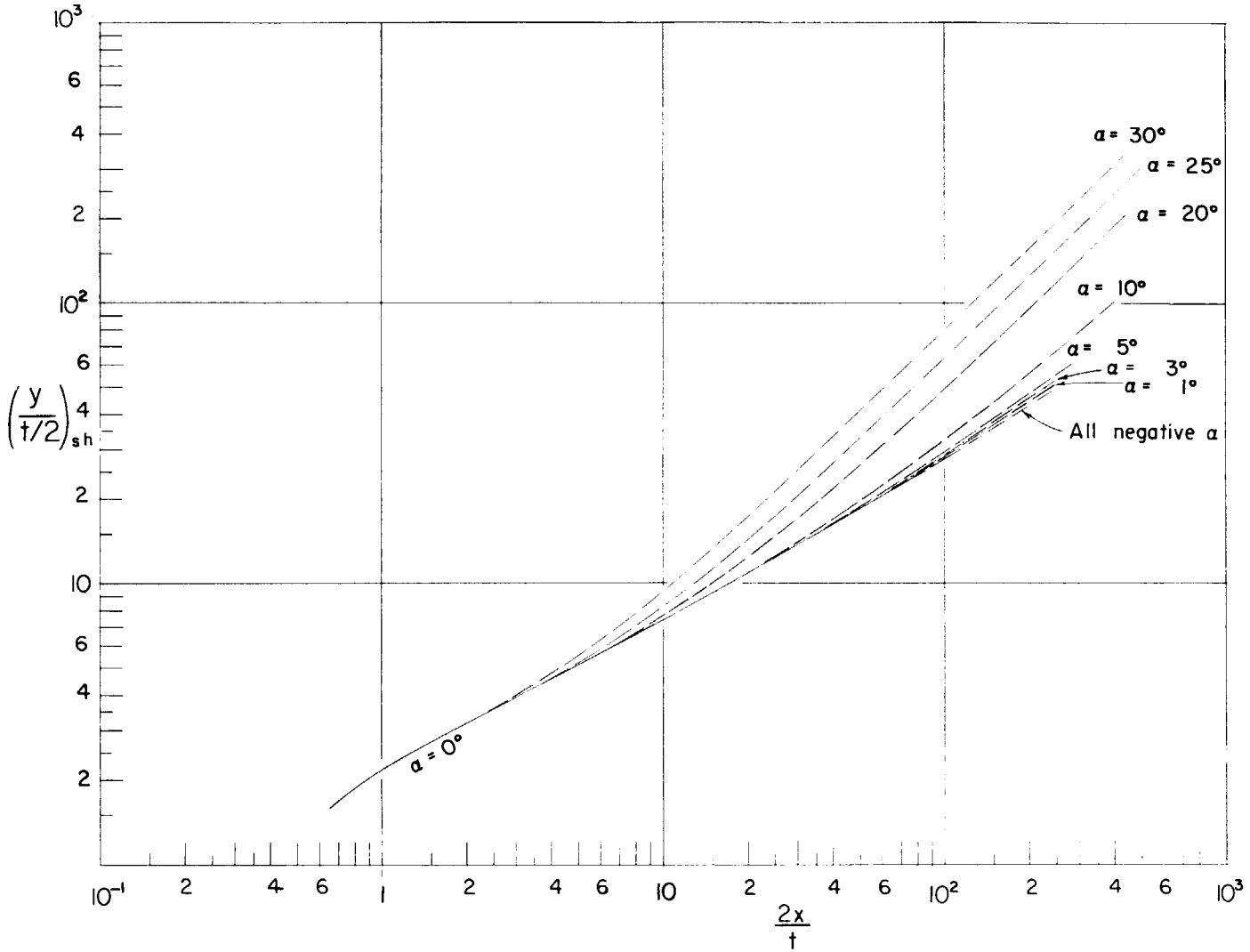

Figure 5.- Shock shape for blunt leading-edge slab through a range of angle of attack. $M_\infty = 20$; $\gamma = 7/5$.

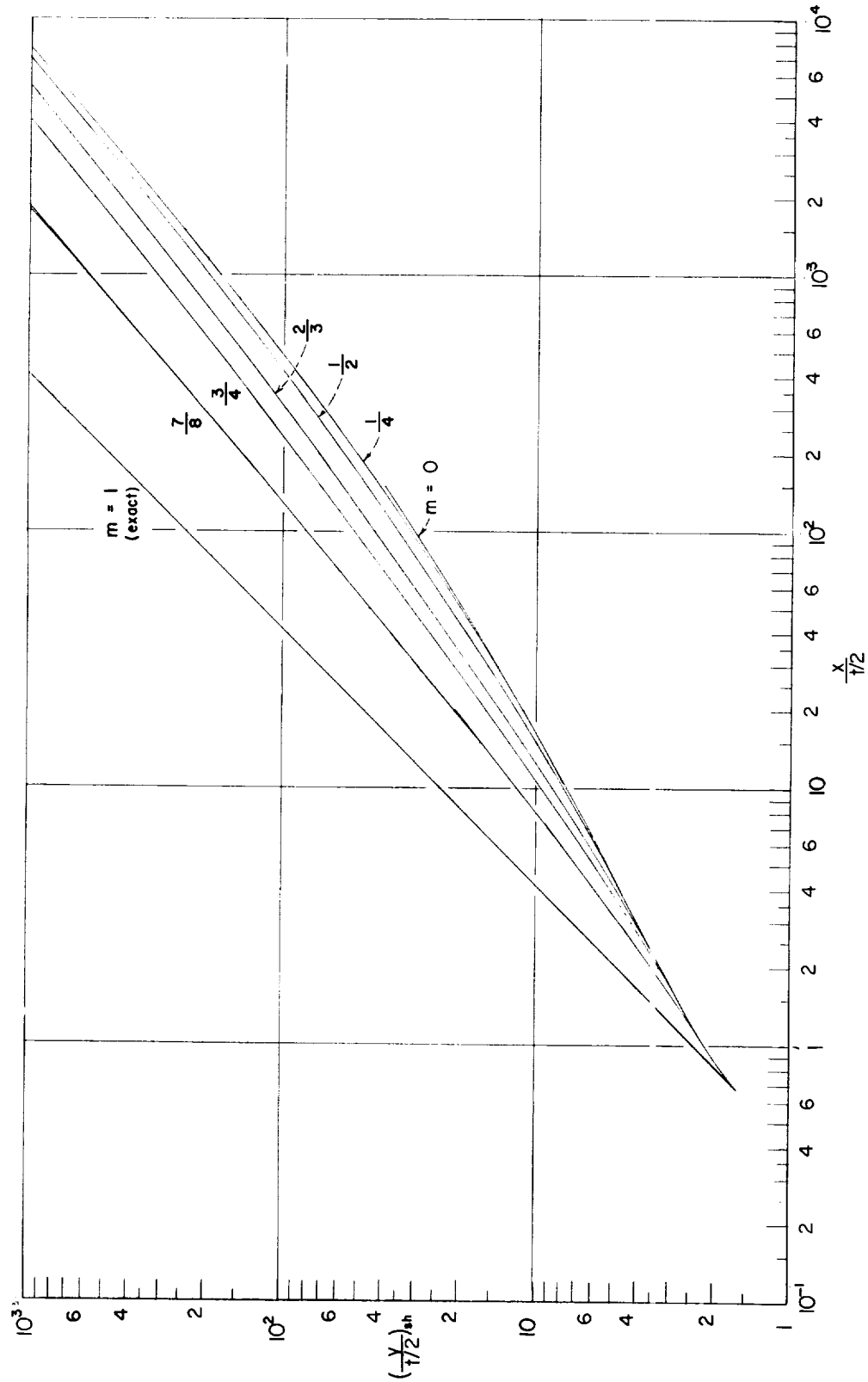

(a) $M_\infty = 10$; $\gamma = 7/5$.

Figure 6.- Effect of power-profile shape on shock shape.

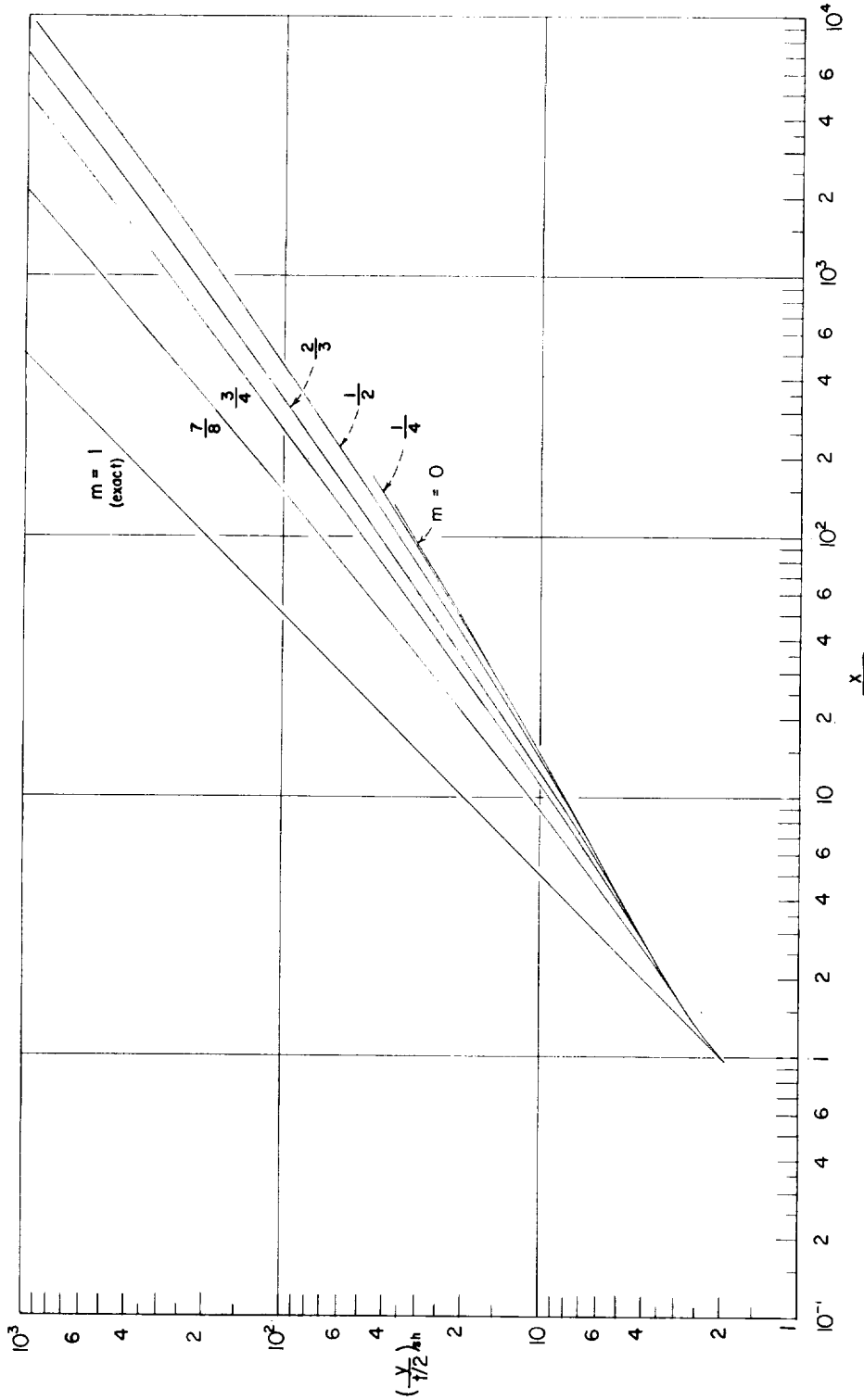

(b) $M_\infty = 20$; $\gamma = 5/3$.

Figure 6.- Concluded.

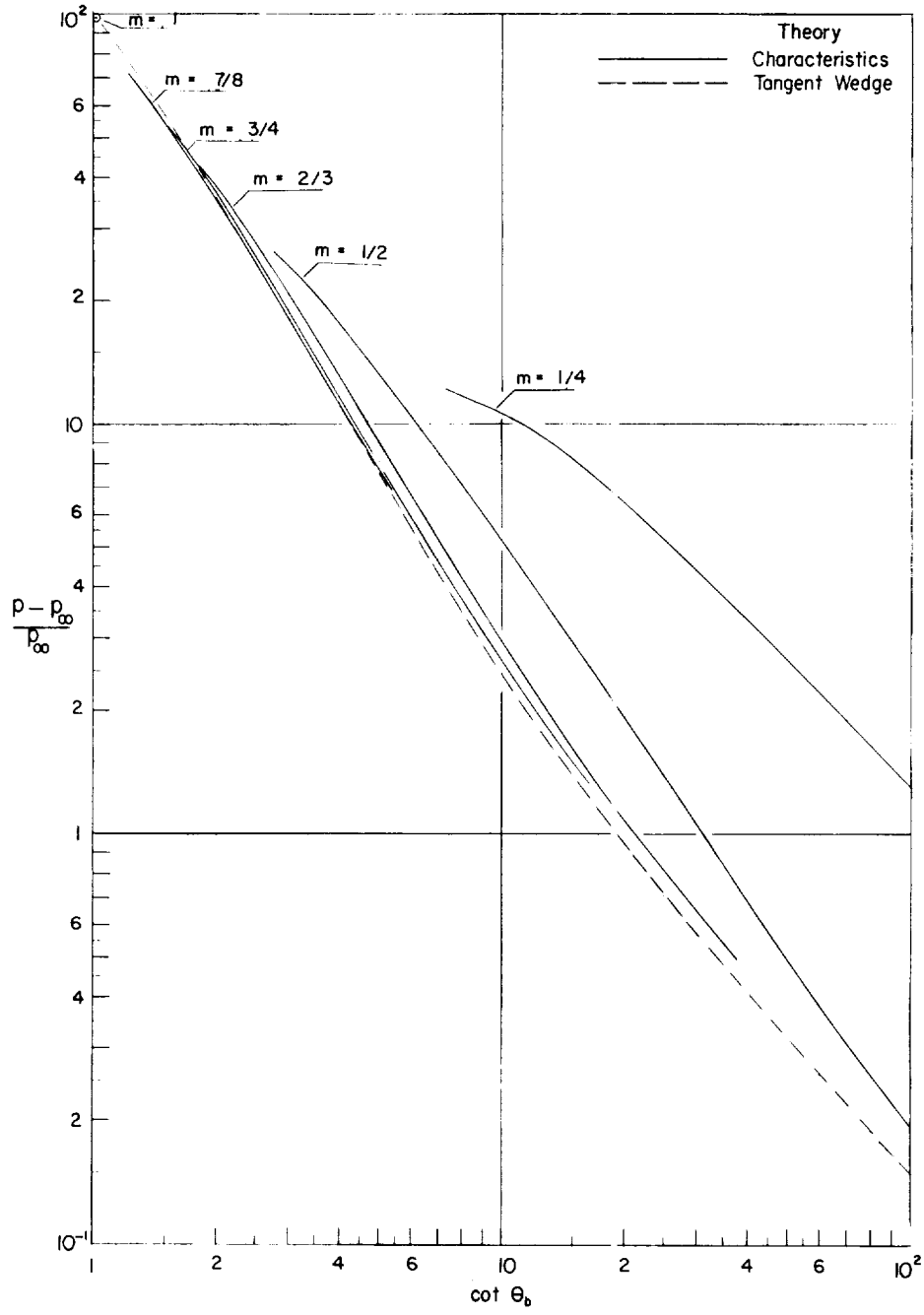

(a) $M_\infty = 10$; $\gamma = 7/5$.

Figure 7.- Pressures on the surface of the power profiles as a function of the reciprocal of the body slope.

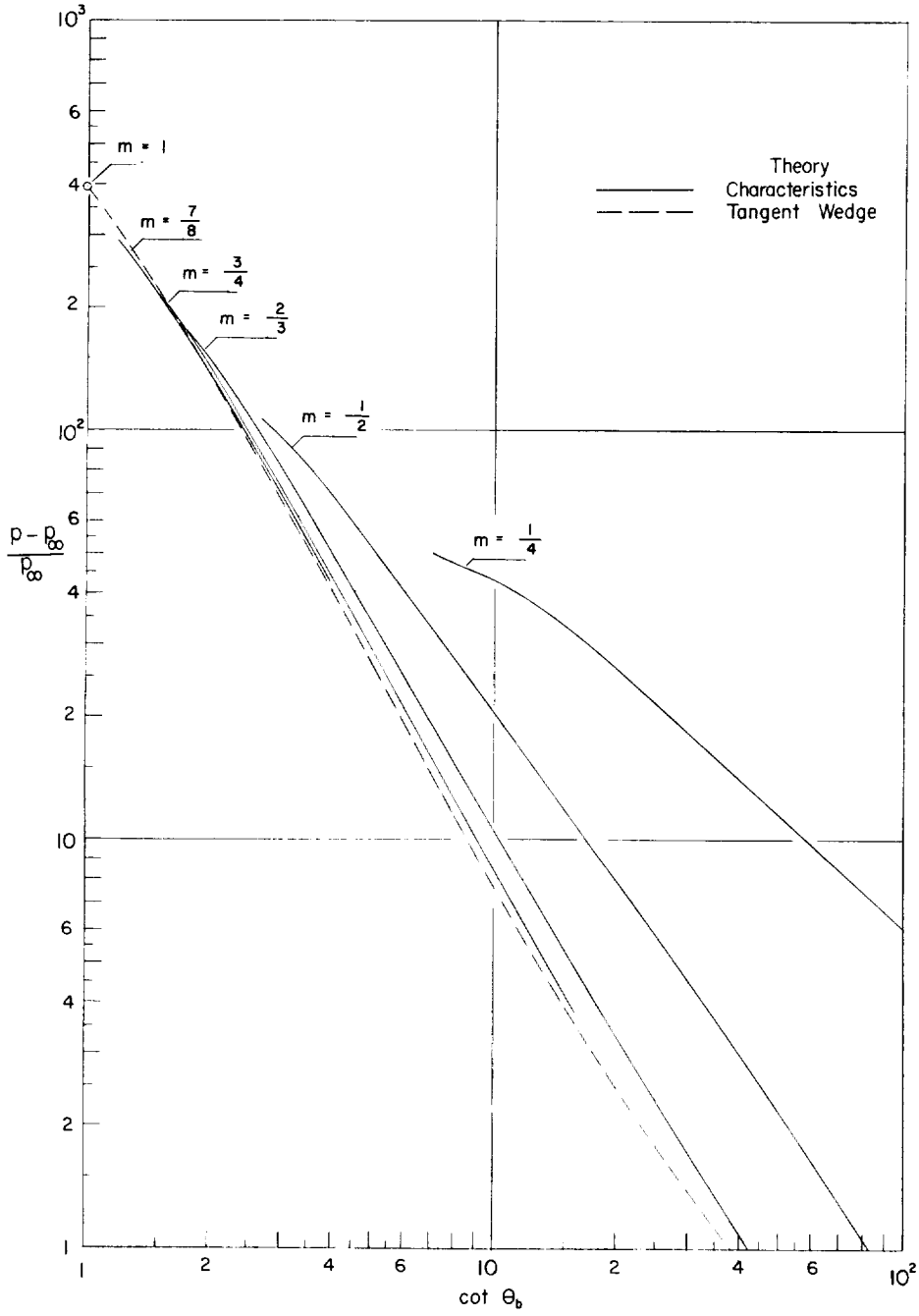

(b) $M_\infty = 20$; $\gamma = 7/5$.

Figure 7.- Continued.

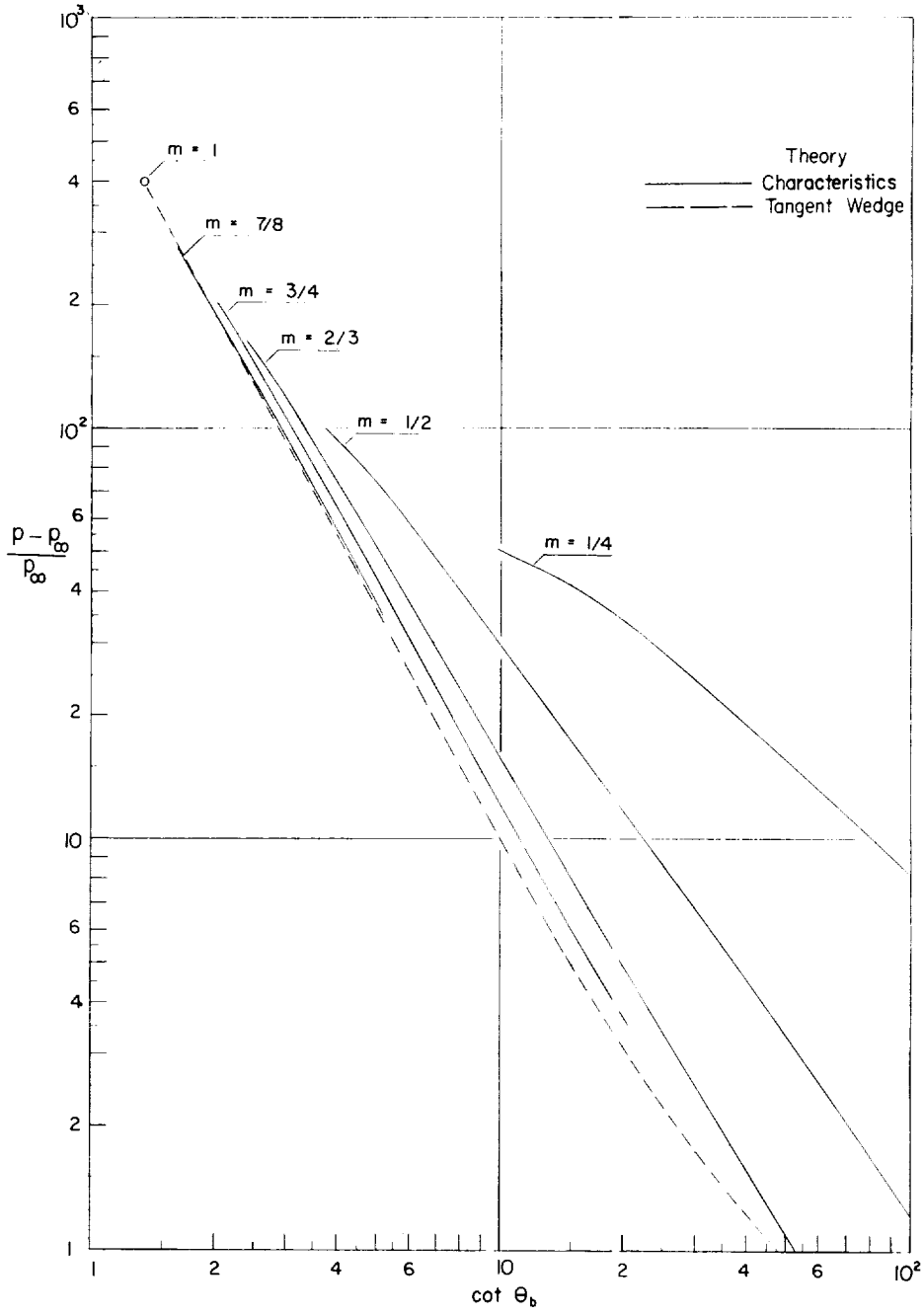

(c) $M_\infty = 20$; $\gamma = 5/3$.

Figure 7.- Concluded.

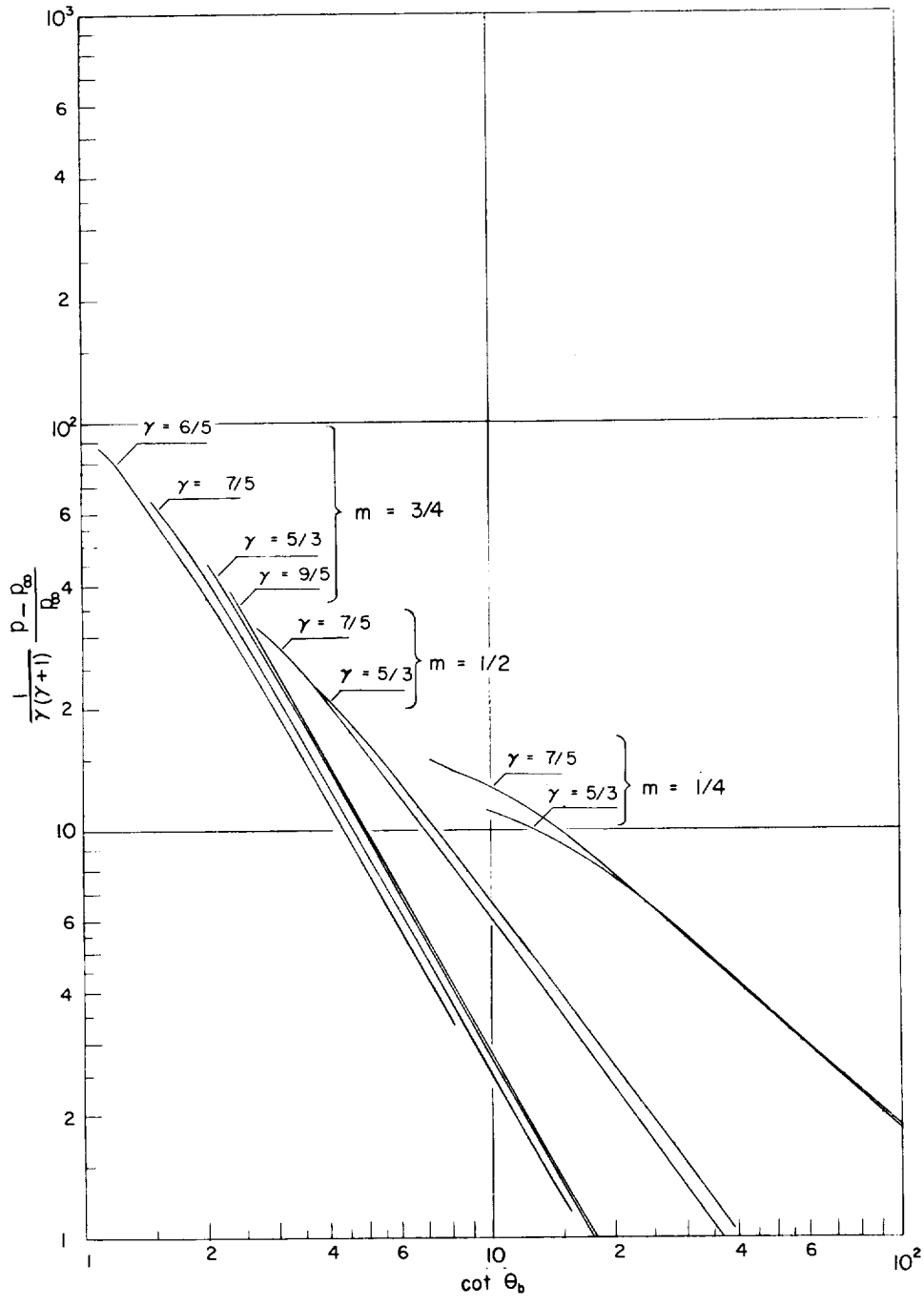

Figure 8.- First-order correlation of the effect of the ratio of specific heats on the pressure distribution on power profiles. M_∞ = 20.

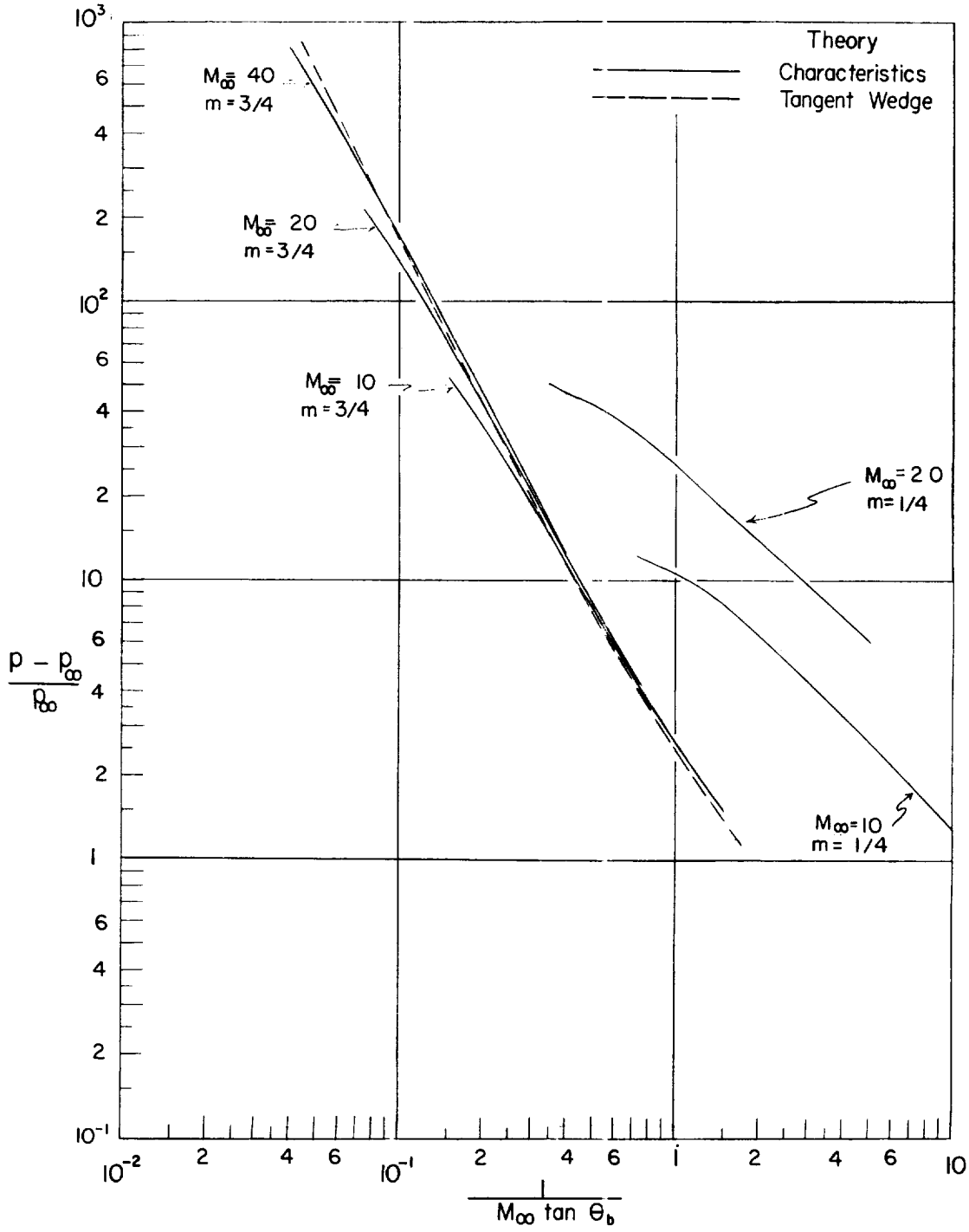

Figure 9.- Correlation of pressures on power profiles according to hypersonic similarity. $\gamma = 7/5$.

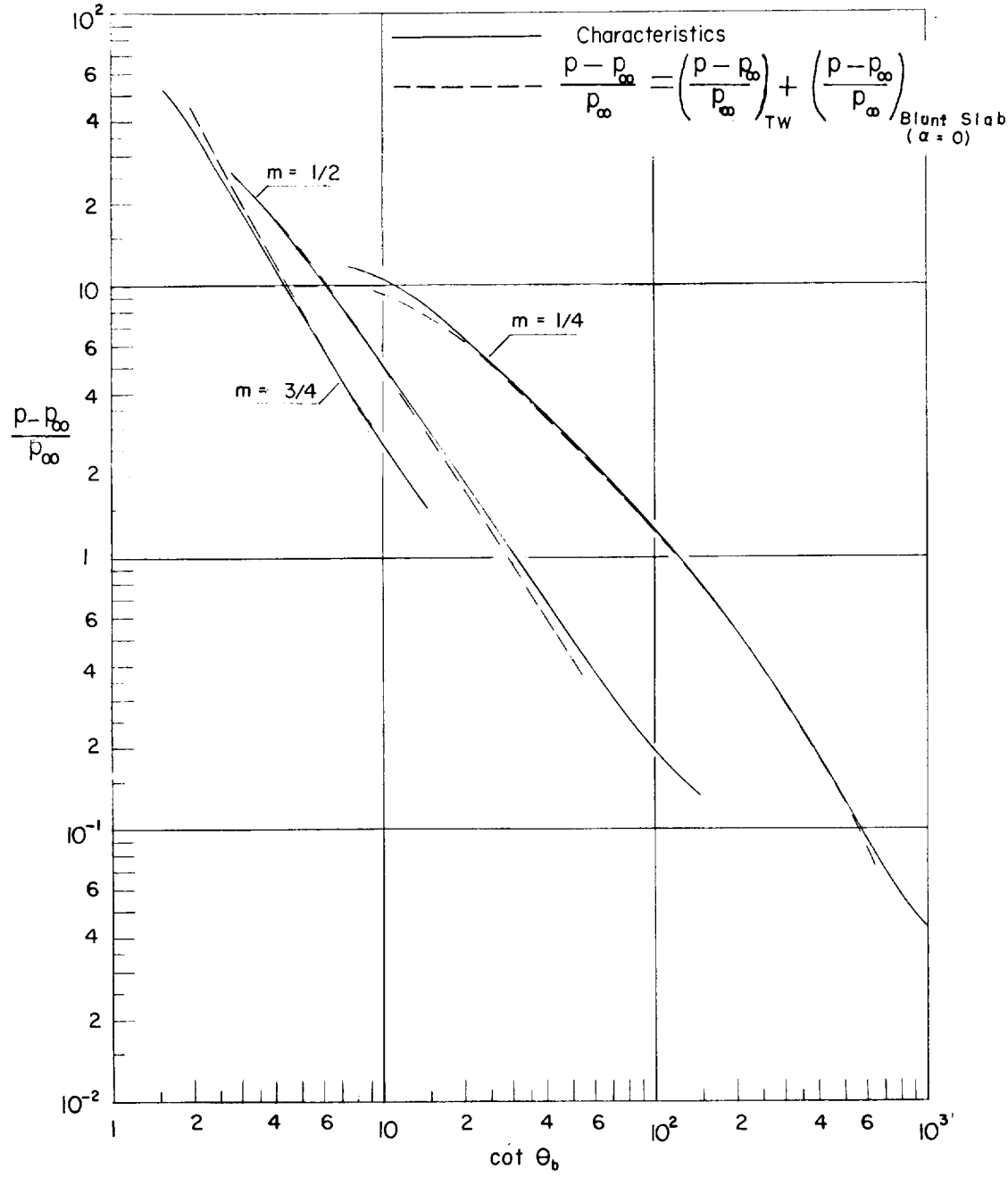

(a) $M_\infty = 10$; $\gamma = 7/5$.

Figure 10.- Prediction of pressures on power profiles by the linear addition of blunt leading-edge induced effects and tangent-wedge theory.

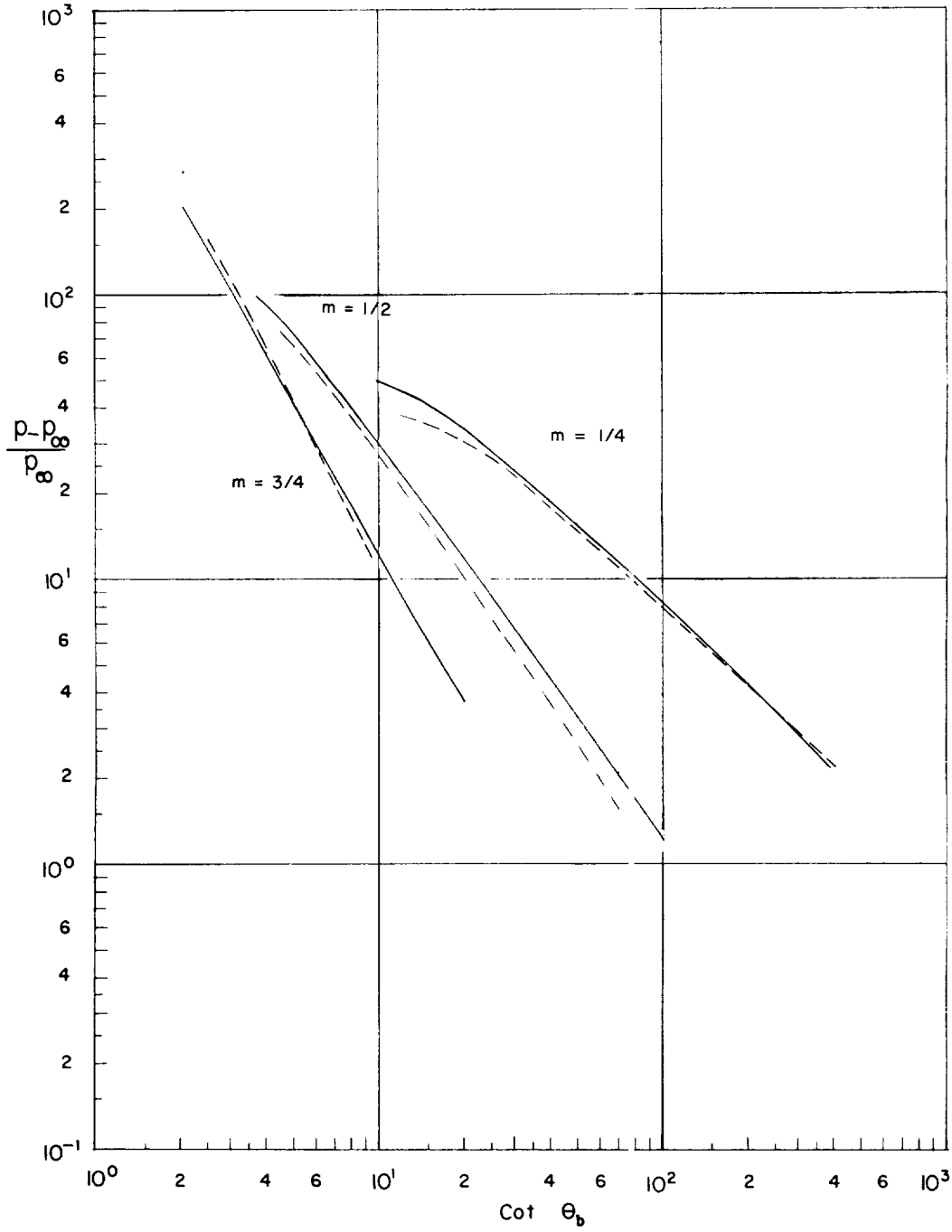

(b) $M_\infty = 20$; $\gamma = 5/3$.

Figure 10.- Concluded.

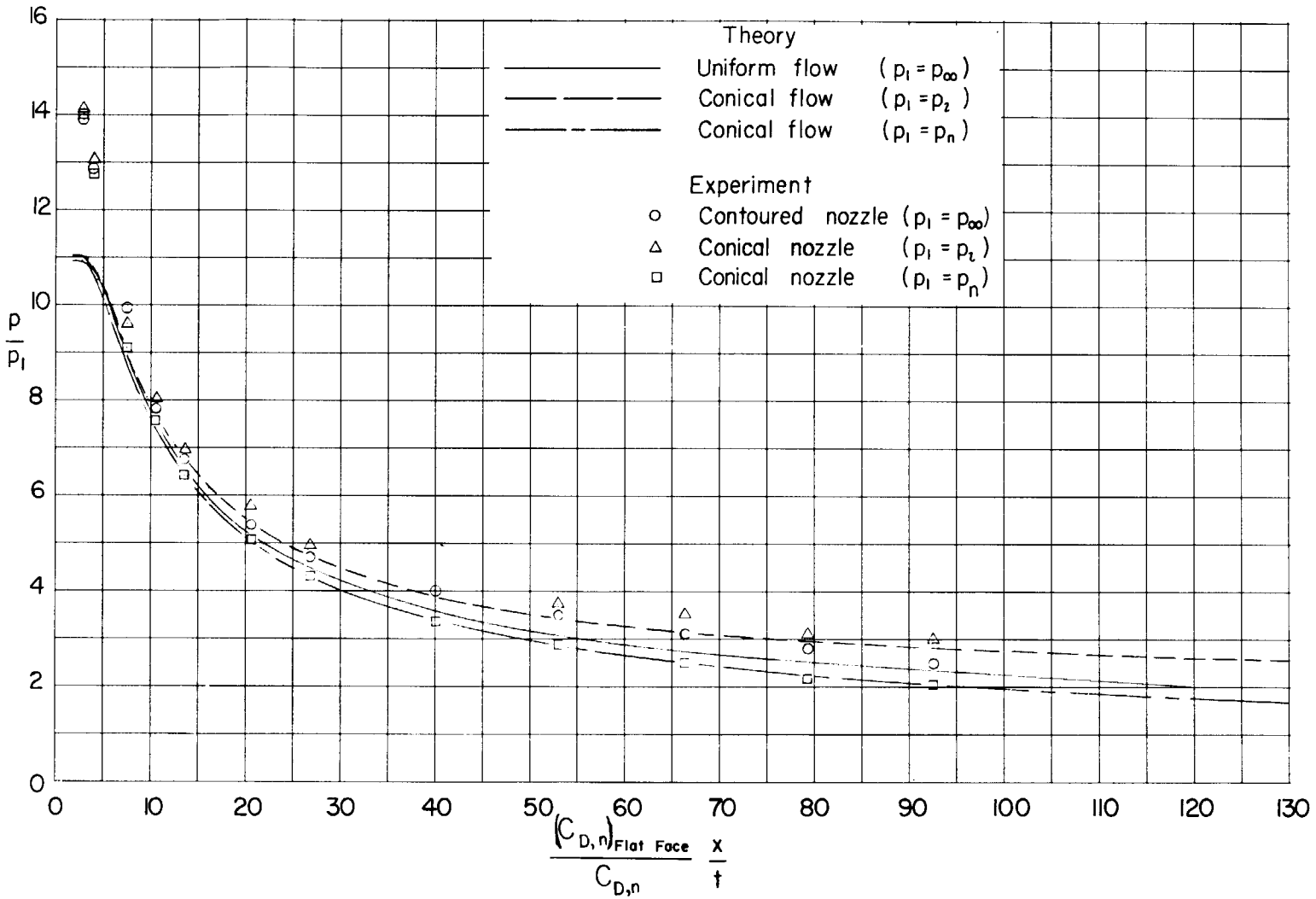

Figure 11.- Comparison of predicted effect of nozzle pressure gradient with data from reference 15 for pressures on a blunt-leading-edge slab. $M_\infty = M_n = 11.6$; $M_n' = 0.012$; $\alpha = 0^\circ$.

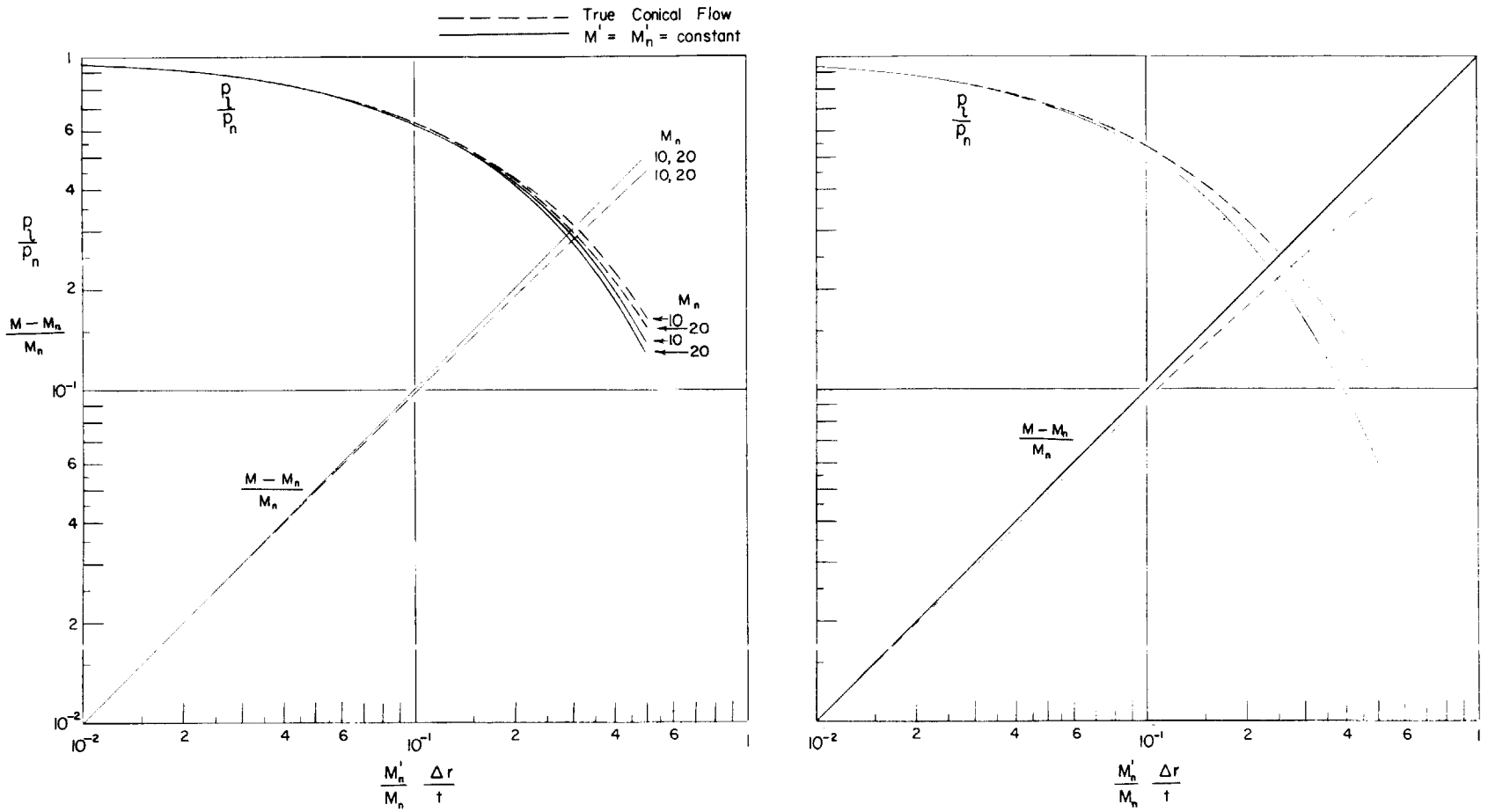

(a) M_n = 10 and 20; γ = 5/3.

(b) M_n = 20; γ = 7/5.

Figure 12.- Comparison of true conical-source-flow Mach number and pressure gradients with those for a linear Mach number gradient along a streamline.

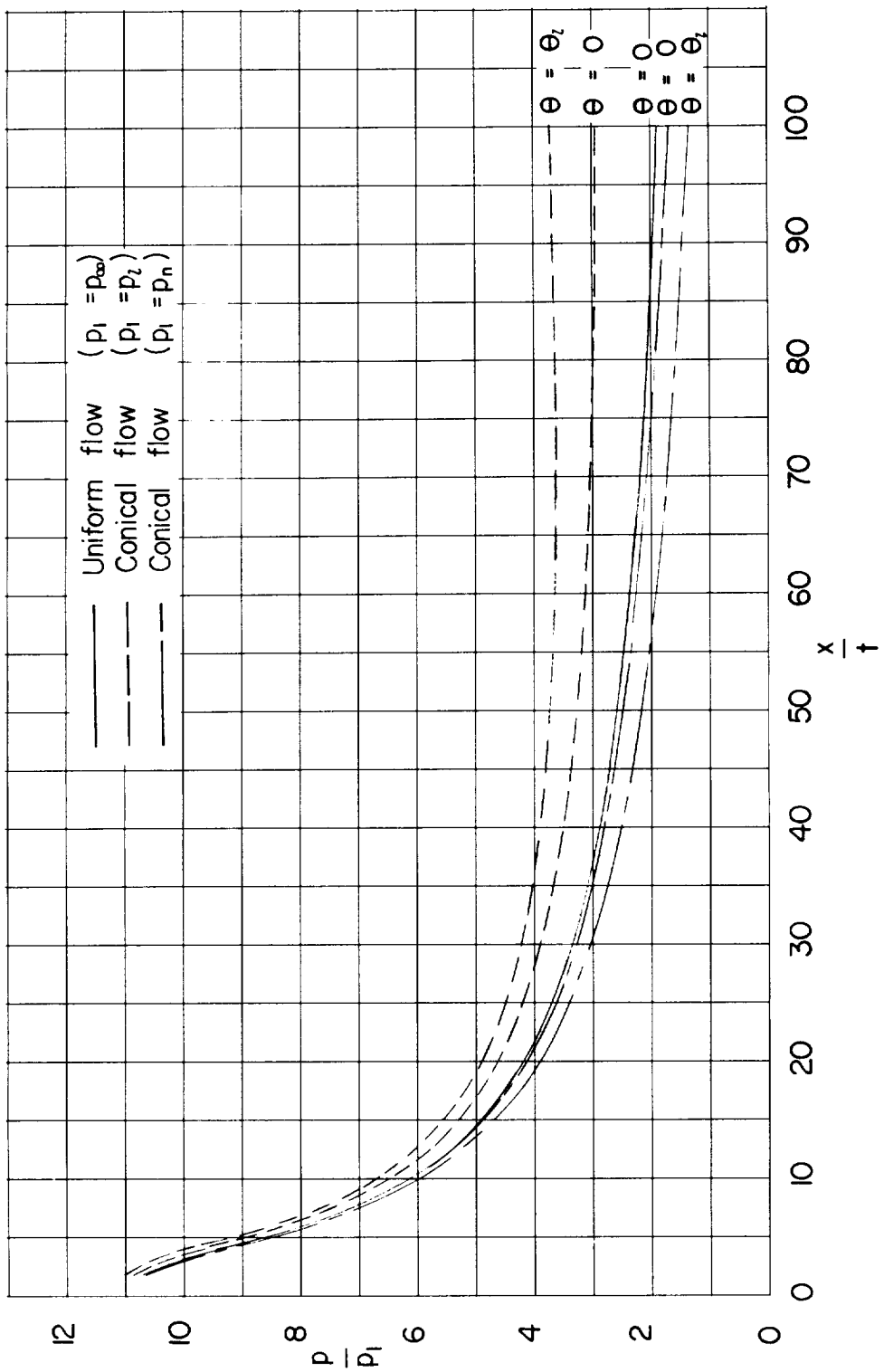

Figure 13.- Effect of including stream divergence in the characteristics solutions for surface pressures on a blunt-leading-edge slab in a source flow. $\alpha = 0^\circ$; $\gamma = 5/3$; $M_n = 11.5$; $M_n' = 0.02$.

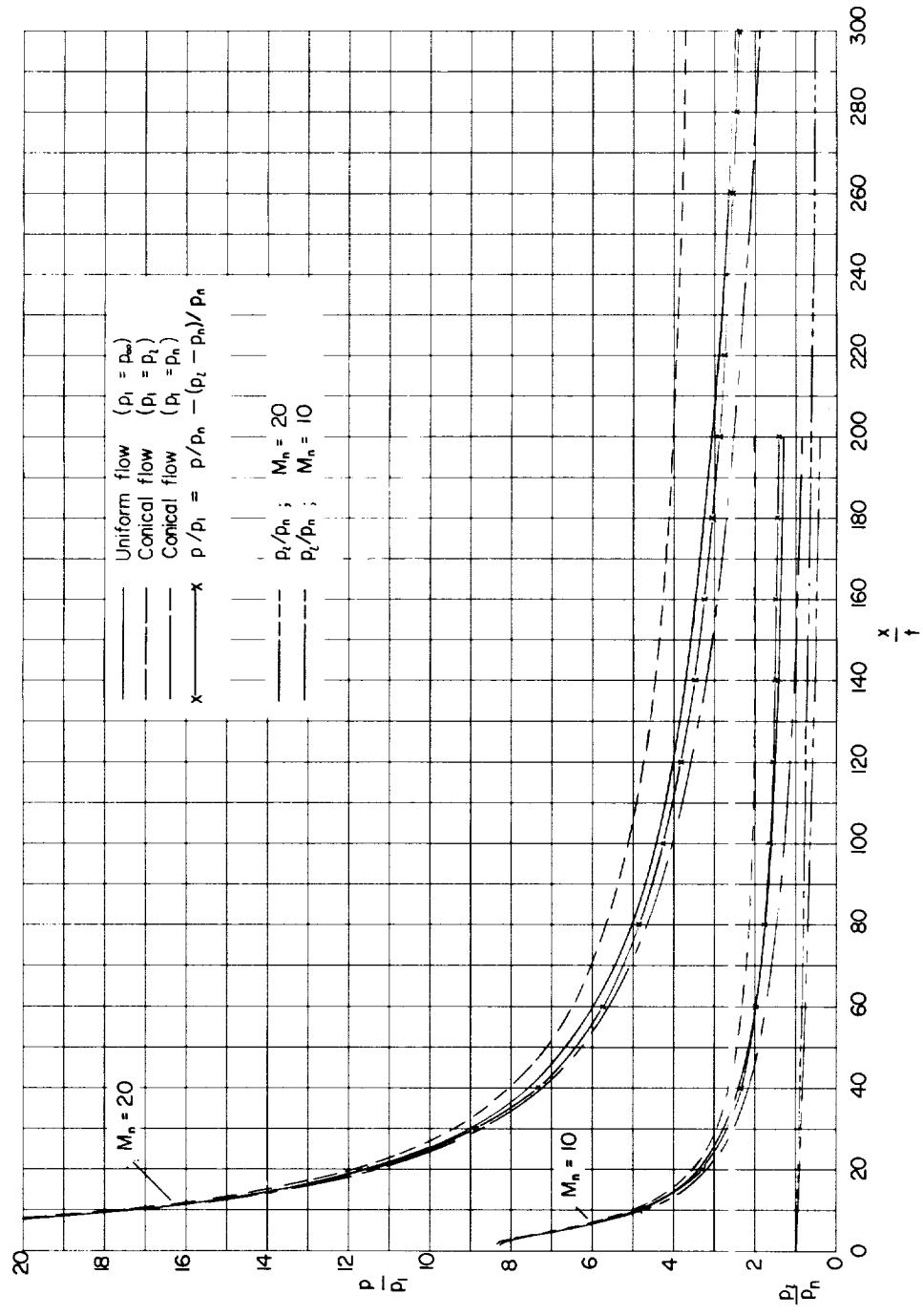

(a) $M_n' = 0.01$; $M_n = 10$ and 20.

Figure 14.- Effect of external pressure gradient on the surface pressures on a blunt-leading-edge slab at zero angle of attack; $\gamma = 5/3$.

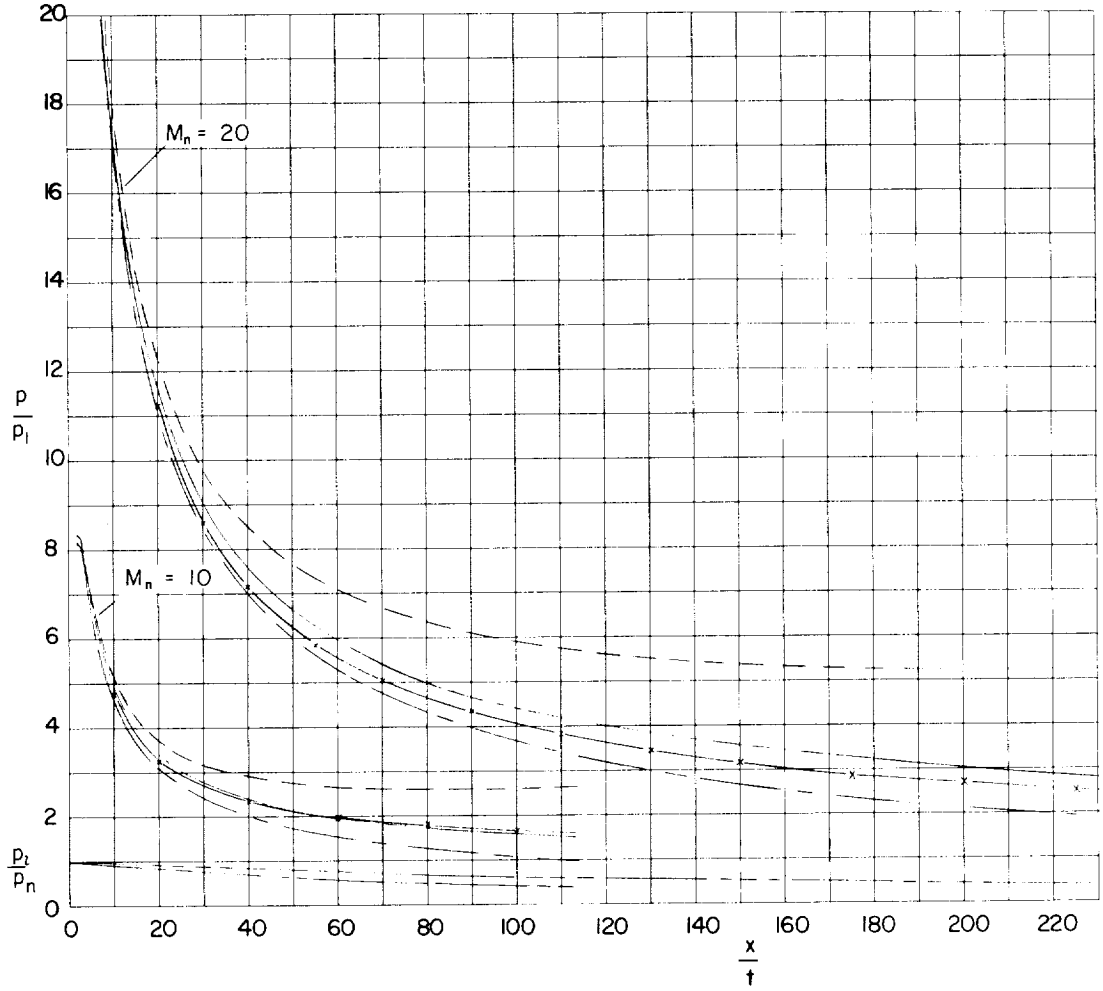

(b) $M_n' = 0.02$; $M_n = 10$ and 20.

Figure 14.- Continued.

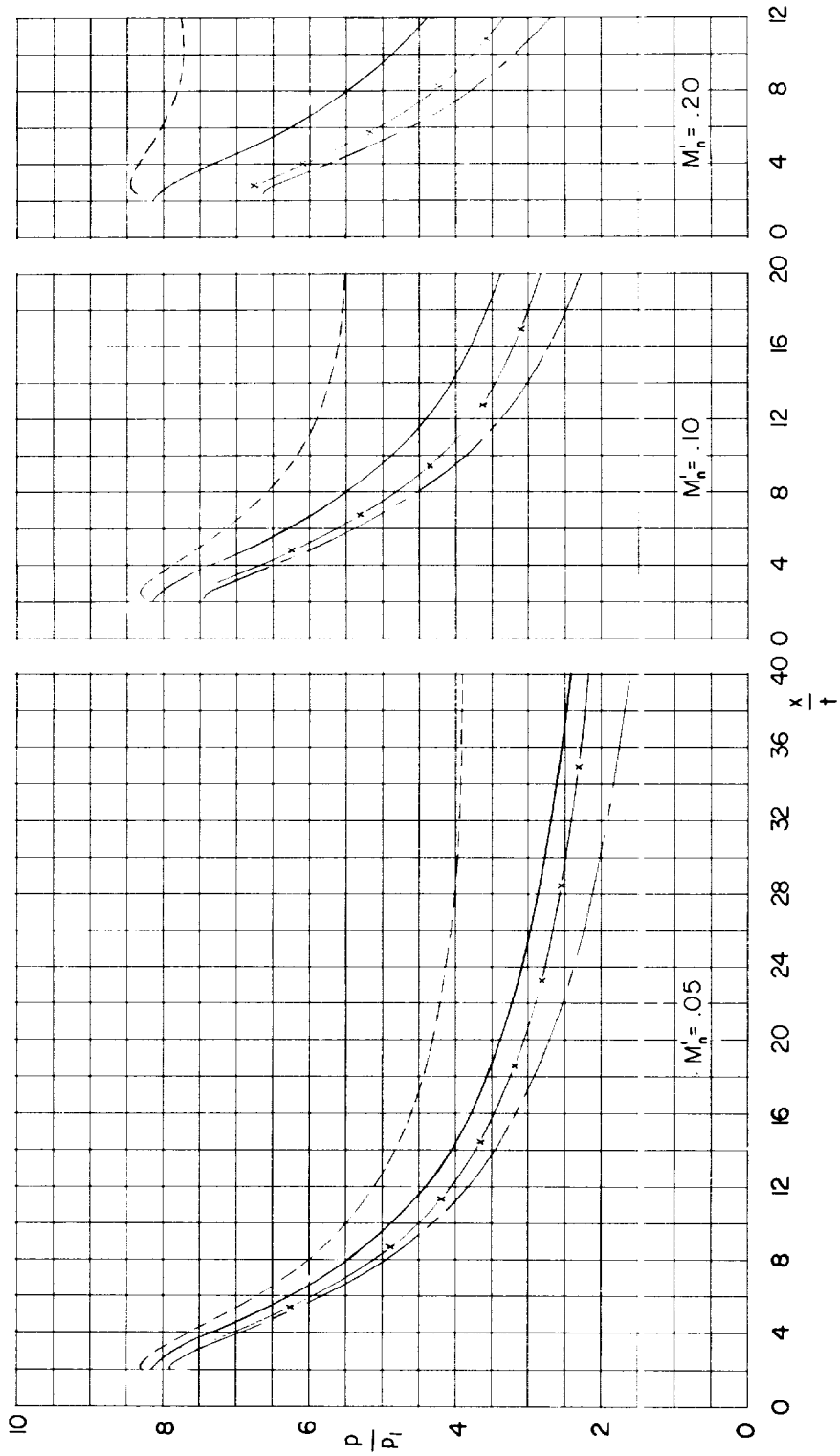

(c) $M_n' = 0.05$, 0.10, and 0.20; $M_n = 10$.

Figure 14.- Continued.

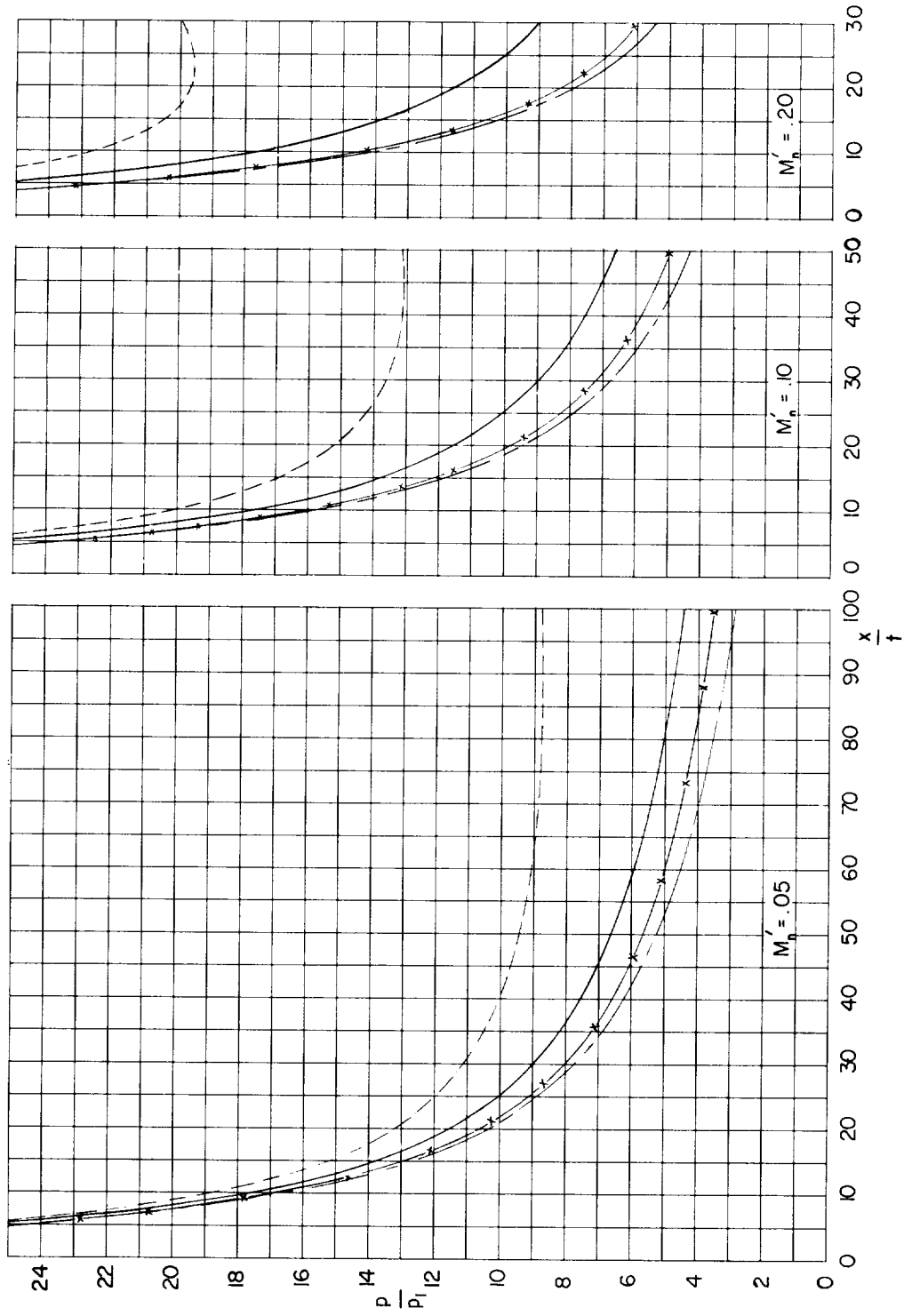

(d) $M_n' = 0.05$, 0.10, and 0.20; $M_n = 20$.

Figure 14.- Concluded.

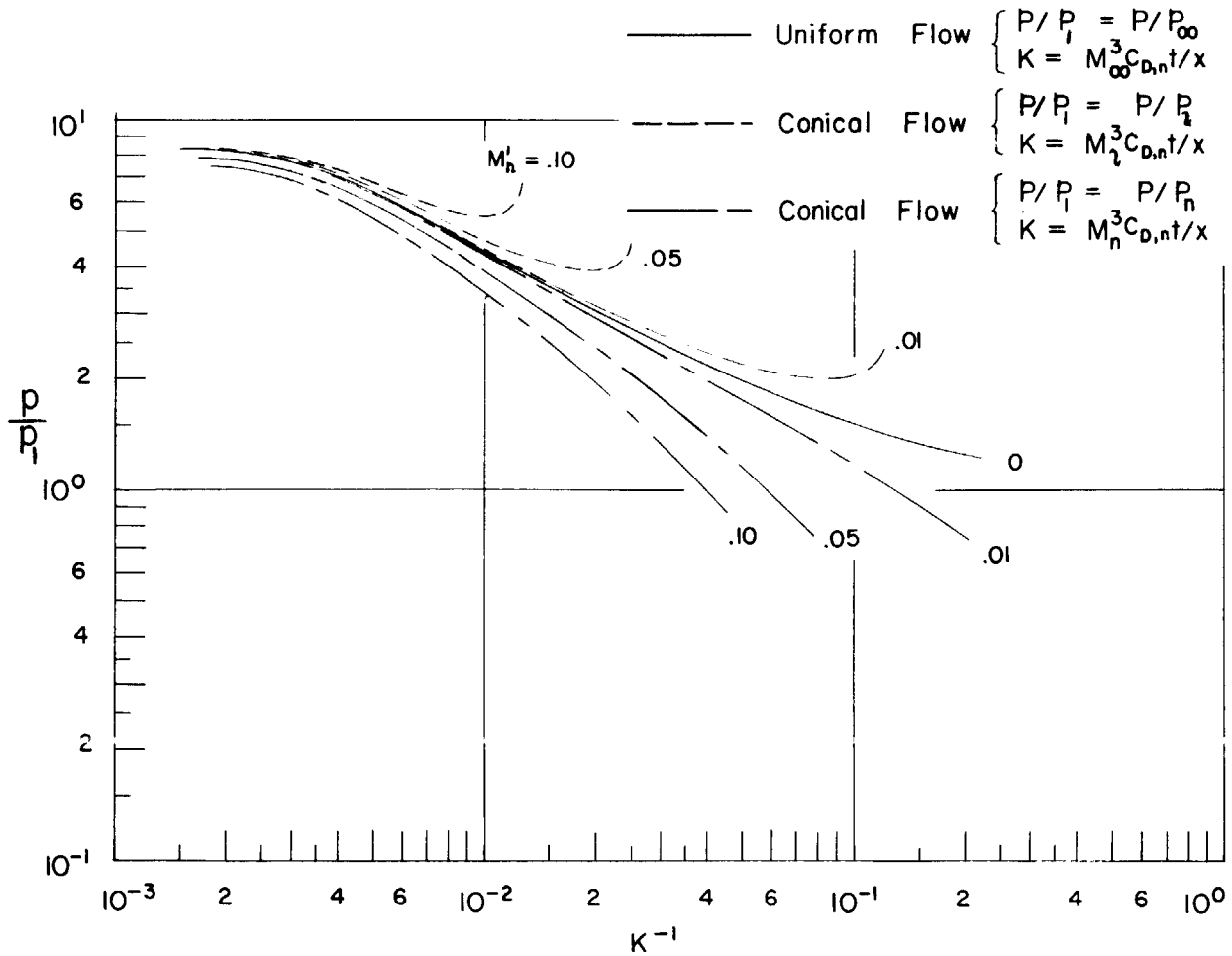

(a) $M_n = 10$.

Figure 16.- Correlation of nonuniform-flow results on the basis of the parameters of blast-wave theory. $\gamma = 5/3$; $M_n' = 0$, 0.01, 0.05, and 0.10.

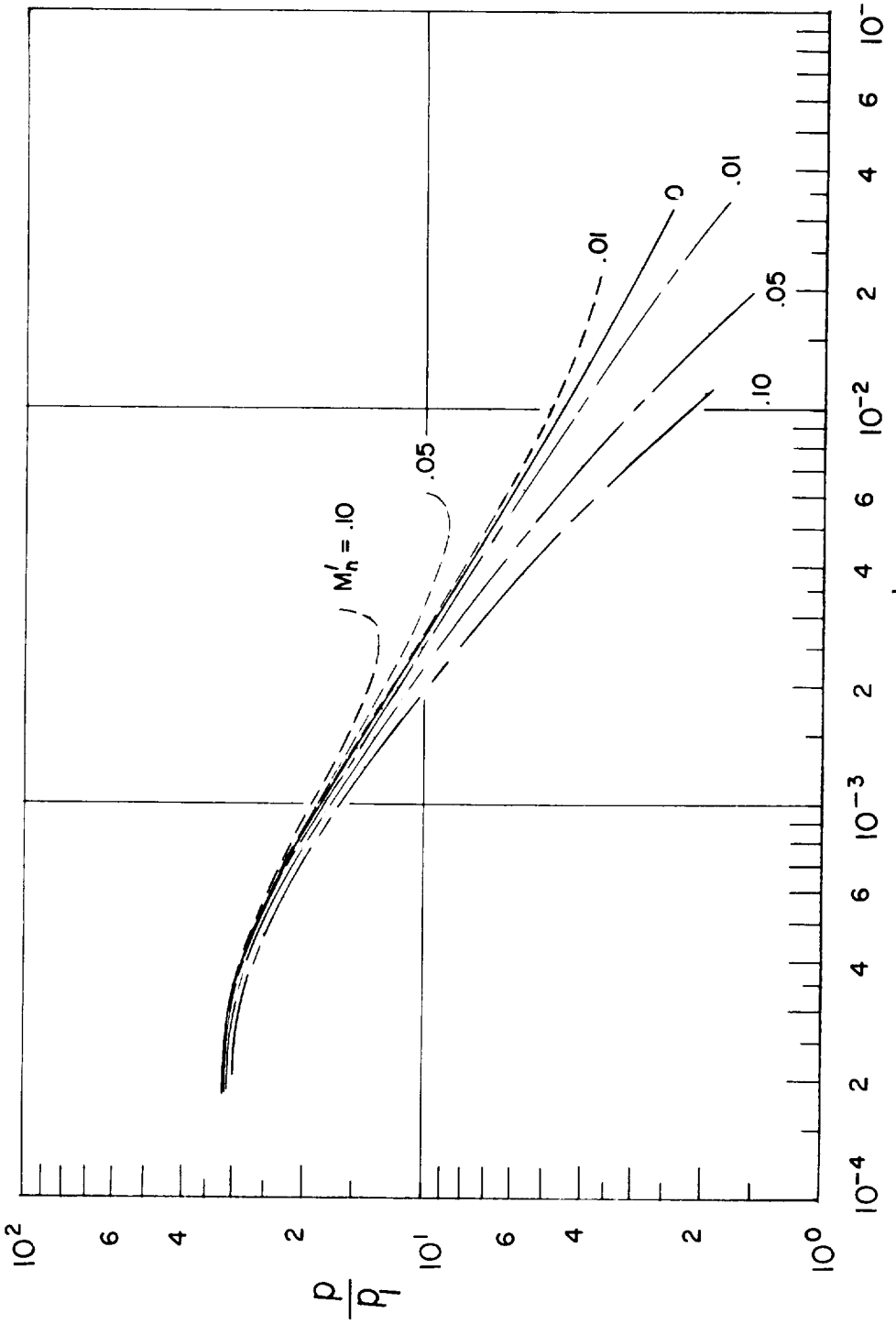

(b) $M_n = 20$.

Figure 16.- Concluded.

L-897